NATIONAL ADVISORY COMMITTEE FOR AERONAUTICS

TECHNICAL NOTE 4002

INTERACTION OF MOVING SHOCKS AND HOT LAYERS

By Robert V. Hess

Langley Aeronautical Laboratory
Langley Field, Va.

NACA
Washington
May 1957

NATIONAL ADVISORY COMMITTEE FOR AERONAUTICS

TECHNICAL NOTE 4002

INTERACTION OF MOVING SHOCKS AND HOT LAYERS

By Robert V. Hess

SUMMARY

This paper treats the interaction between hot layers extended along the wall and normal or oblique shocks moving over them. Emphasis is on the cases of large hot-layer temperatures and strong shock waves for which small-perturbation theories are not applicable. A variety of possible interaction patterns are described. Of greatest interest are the more extreme cases when the hot layer is forced to accumulate in a growing bubble-like region bound to the moving shock, and some of the cold air above the layer moves around the bubble and interposes a high-speed forward-moving cold jet between the wall and the bubble. For some cases, especially with oblique shocks, this reverse jet may not form. Mixing will eventually limit the size of the bubble and make its characteristics more nearly like those of the more familiar separation bubbles. The effects of viscosity at the wall remains essentially different, however, since the shock is moving relative to the wall.

Many other details and characteristics of the interaction pattern, such as the decay of the interaction effects along the hot layer and along the hot layer with the interposed cold jet below it and the shape of the normal shock far above the main interaction region, are described and discussed.

INTRODUCTION

The interaction of a blast wave with a hot layer covering a wall has been given considerable attention within recent years. The major emphasis has been on the shock refraction patterns occurring for layers of comparatively small excess temperatures. (See, for example, ref. 1.) As pointed out in the present paper, however, for layers of large excess temperatures and for strong incident shocks, the hot-layer shape undergoes such drastic changes that small-perturbation theories become incapable of even suggesting the phenomenon. The reason is that, for the large excess temperatures, the density of the hot layer is so low that the pressure rise across the shock is more than sufficient to accelerate the hot layer to the speed of the shock itself; accordingly, the hot layer will have to accumulate in a growing hot bubble-like region bound to the moving shock.

Another effect that may be associated with the bubble formation is that part of the cold outer air may run under the bubble and interpose itself between the wall and the hot layer. The theoretical basis for the formation of the bubble-like regions in the hot layer was initially outlined by the author in an unpublished note to Griffith and Bleakney of Princeton University, who subsequently developed an ingenious experimental approach which permitted the confirmation of the existence of such regions. (See ref. 2.) A large part of this paper deals with this bubble development.

In contrast with the case of a plane shock, mathematical analysis of the interaction pattern produced by a spherical shock meets with many difficulties even when the excess temperature of the hot layer is so small and the incident shock is so weak (ref. 3) that small-perturbation methods can be used. It is evident that the difficulties will be much greater when strong shocks and large excess temperatures of the hot layer are considered since nonlinear and transonic effects are encountered in addition to unsteady effects. Accurate analysis of these strong interactions would most likely require a numerical approach with the attendant disadvantage that each interaction case would have to be considered separately.

Accordingly, the analysis of the present paper is based on two basic simplifications or idealizations of the physical problem. First, the spherical shock has been replaced with a plane shock, either normal or oblique, of constant strength. Second, the hot layer is considered to be of uniform thickness and uniform temperature, with a sharp temperature discontinuity at the boundary between it and the cold air above it. Both simplifications tend to reduce the time-dependent interaction problems to steady-flow problems, which are much easier to analyze. (Some discussion of the order of magnitude of the time required for the decay of the transient effects is given subsequently.) Even for these simplified steady-flow cases, however, the transonic and nonlinear characteristics still exist; therefore complete solutions would be very difficult. The approach adopted was first to classify the possible interactions into several fundamentally different types and to determine the ranges of conditions corresponding to each type and then to discuss the major characteristics of each type. For this purpose the patterns of reference 4, although not concerned with hot layers, offered useful guidance. Studies of cavitation flows (for example, ref. 5) were useful in understanding the flow over the bubble.

The analysis is mainly concerned with the interaction of a hot layer with a normal shock. Six different types of interaction are described. In four of these types the hot layer experiences bubble formation; in the other two types the hot layer is not terminated by a bubble and is referred to hereafter as the "throughgoing hot layer." The interaction with oblique shocks is discussed and some considerations of spherical shocks are included. A large number of interaction types may exist

because of the great variety of refraction patterns connected with various incidence angles of the oblique shock, even for small excess temperatures in the hot layer (see ref. 1); however, the discussion is limited only to the most significant types of phenomena. The greater part of the paper makes use of ideal flow considerations, but the effects of viscosity and mixing are included in a brief section.

Three appendixes have been included in order to study the decay of the interaction effects along the directions away from the region of the largest concentration of the effects. In this manner, an estimate can be made of the size of the region involved in the interaction pattern. For an analysis of these asymptotic decay effects a small-disturbance approach can be used. Appendix A is a study of the decay of the interaction between an infinite supersonic stream and a hot layer. It applies to the asymptotic decays upstream of normal shocks and both upstream and downstream of oblique shocks interacting with the hot layer. Appendix B concerns the asymptotic shape of the deformed normal interacting shock above the region of large hot-layer distortion and also discusses the asymptotic decay of this hot-layer distortion behind the interaction zone where the flow is subsonic. Appendix C treats the asymptotic behavior of the cold jet of air which may be forced to move under the bubble of the hot layer for some of the interaction types. Some of the problems treated in the appendixes have aspects in common with jets embedded in moving streams. It is the aim of the appendixes to present the decay effects in their simplest mathematical form. Some of the results could have been obtained by starting with published small-disturbance calculations for a complete interaction field and by reducing the results to the desired asymptotic decay effects; however, the mathematical simplicity of the present treatments should help the reader to attain better physical insight into the phenomenon.

SYMBOLS

A, A^* B, B^* C, C^*, C^{**}	constants
a	speed of sound
M	Mach number, u/a
p	pressure
s	decay modulus

T	temperature
t	time
u	horizontal velocity component
v	vertical velocity component
x	horizontal coordinate
y	vertical coordinate
α	Mach angle
γ	ratio of specific heats
ϕ	small-disturbance potential

Subscripts:

c	cold
cr	critical
h	hot
j	reverse jet
o	stagnation condition
1	undisturbed flow
2	flow behind incident normal shock
3	flow over bubble boundary

TYPES OF STEADY-FLOW INTERACTIONS WITH NORMAL SHOCK

Assumptions Underlying Steady Flow in Layer of Constant Height and Damping of Initial Transient-Flow Effects

The interaction pattern associated with a moving shock is steady with respect to an observer moving with the shock provided that the shock does not change strength or shape during its motion. This fact is valid for a normal shock moving in a channel of constant cross section.

Consider a normal shock moving along a wall and interacting with a hot layer that begins somewhere along the wall. (See fig. 1.) As the shock hits the hot layer, another shock will move ahead into the hot layer. During the initial period in which the front-running shock moves through regions of changing height of the hot layer, the shock changes its speed and strength; but as it approaches the region where the hot layer attains constant height, its speed tends to become uniform. In order to establish steady flow relative to the interacting shock, it is not enough that the shock moving in the hot layer attains constant speed; the shock must also have the same speed as the interacting shock. These conditions are made possible because the hot-layer boundary gives way to the pressure increase across the shock moving through it and slows the shock down to the speed of the main shock. Steady flow relative to the interacting normal shock is attained when the change in pressure and velocity inside the hot layer produced by the shock and the increasing cross section matches the pressure and velocity jump through the interacting normal shock.

The following section shows that conditions also exist for which the steady pressure and velocity changes through the interacting shock are matched by an entirely subsonic steady flow having no shock in the hot layer. The fact that the buildup of the steady flow requires a front-running shock, but not the steady flow itself, may appear somewhat strange to the blast expert, who makes less use of the steady-flow concepts than the aerodynamicist. For purposes of illustration, consider the acceleration of an airfoil to constant speed. During the acceleration, compression waves or shocks move ahead of the airfoil. These decaying waves and their reflections are necessary to establish the steady subsonic flow relative to the airfoil; the steady flow itself, however, no longer contains a shock.

A rough estimate of the time required for the damping of the initial transient effects may be of interest. Dimensional reasoning suggests that the time to approach steady flow should depend on the ratio of the hot-layer height to some speed that indicates the rate of this approach. In an unsteady flow buildup, both the downstream waves and the upstream waves play a part. The upstream waves traveling at a speed given by the absolute difference between the speed of sound a and the average flow speed $\overline{u}$ are the slower ones and thus give a better estimate of the speed of approach to steady flow. Consequently, where regions of high supersonic steady flow (for example, Mach number 2) or low subsonic flow are approached in the interaction pattern, the time for the establishment of such flows should be of the order of the hot-layer height divided by the speed of sound, whereas the attainment of approximately sonic flow would take longer. Note that these estimates refer to the times required for the damping of the transient effects to practically negligible values. This fact is especially significant in the interpretation of the damping time of disturbances in subsonic flow. Since subsonic disturbances can

move both upstream and downstream, the damping of progressively weakened reflected and rereflected waves over a certain length would theoretically take infinitely long. For practical purposes, however, the damping occurs roughly at a rate $\bar{u} - a$. Experience with other starting problems as, for example, those that occur in wind-tunnel operation (ref. 7) shows that dimensional considerations of this type yield generally adequate results.

Classification of Steady-Flow Interactions into Six Types

The approach of steady flow which is the basis of the classification is briefly explained. The state before the interaction is given in figure 1. For the steady-flow approach it is convenient to use a shock-bound reference system. (See fig. 2.) In the steady-flow system moving with the shock, the undisturbed regions of the cold air and the hot layer move at the same relative speed u_1. The pressure across the hot-layer boundary is continuous, and thus the pressures in these two regions are the same. The first step in the classification is to differentiate between those cases in which the undisturbed hot-layer flow is supersonic and those in which it is subsonic, in other words, to differentiate between those cases in which the hot layers contain shocks and those cases in which no shock exists on the hot layer. Inasmuch as the velocities in the undisturbed hot and cold regions are the same but the temperatures differ, the Mach numbers

$$M_{1h} = \frac{u_1}{a_{1h}}$$

and

$$M_{1c} = \frac{u_1}{a_{1c}}$$

are related by

$$M_{1h}^2 = M_{1c}^2 \frac{T_{1c}}{T_{1h}}$$

When $M_{1h} = 1$,

$$M_{1c}^2 = \frac{T_{1h}}{T_{1c}}$$

This relation thus serves for the desired differentiation and is plotted as M_{1c} against $\frac{T_{1h}}{T_{1c}}$ in figure 3 (the curve that goes through the lower

left corner of the diagram). Points below the curve represent subsonic, and hence shock-free, hot-layer flows; points above the curve represent cases for which the flows in the hot layer involve shocks.

The next step is to differentiate those cases for which the maximum possible pressure rise (to stagnation pressure) in the hot layer is less than the pressure rise through the main shock when the flow in the hot layer must come to rest and accumulate in a bubble or stagnation region at the foot of the shock. For this calculation, one-dimensional-flow relations are used for the hot layer. Some oversimplification is thereby involved inasmuch as the hot-layer shock must deform somewhat from the normal as the boundary is approached because of the deviation of the hot-layer boundary due to the interaction; furthermore, the subsonic flow in the hot layer is modified to varying degrees from the one-dimensional relations.

Proceeding, then with the one-dimensional relations, a dividing line may be constructed in the $M_{1c}, \frac{T_{1h}}{T_{1c}}$ plane of figure 2 in order to separate interactions of the throughgoing type from interactions with a stagnation region. This dividing line may be expressed through the equality of the pressure ratios p_{2c}/p_1 and p_{oh}/p_1. The pressure jump p_{2c}/p_1 through the shock is expressed in terms of the Mach number M_{1c} by the following relation (see ref. 8 for this and subsequent relations):

$$\frac{p_{2c}}{p_1} = \frac{2\gamma}{\gamma + 1} M_{1c}^2 - \frac{\gamma - 1}{\gamma + 1} \tag{1}$$

The expression for the pressure ratio p_{oh}/p_1 in terms of the Mach number M_{1h} in the hot layer depends on whether a shock exists in the hot layer or not. In the case of a hot layer with shock,

$$\frac{p_{oh}}{p_1} = \frac{\left(\frac{\gamma + 1}{2} M_{1h}^2\right)^{\frac{\gamma}{\gamma-1}}}{\left(\frac{2\gamma}{\gamma + 1} M_{1h}^2 - \frac{\gamma - 1}{\gamma + 1}\right)^{\frac{1}{\gamma-1}}} \tag{2}$$

whereas for a hot layer without shock,

$$\frac{p_{oh}}{p_1} = \left(1 + \frac{\gamma - 1}{2} M_{1h}^2\right)^{\frac{\gamma}{\gamma-1}} \tag{3}$$

Equating p_{2c}/p_1 with p_{oh}/p_1 from equation (2) for flow with a shock in the hot layer yields

$$M_{1c} = \sqrt{\frac{\gamma + 1}{2\gamma} \frac{\left(\frac{\gamma + 1}{2} M_{1h}^2\right)^{\frac{\gamma}{\gamma-1}}}{\left(\frac{2\gamma}{\gamma + 1} M_{1h}^2 - \frac{\gamma - 1}{\gamma + 1}\right)^{\frac{1}{\gamma-1}}} + \frac{\gamma - 1}{2\gamma}} \tag{4}$$

Equating p_{2c}/p_1 with p_{oh}/p_1 from equation (3) for shock-free flow in the hot layer gives

$$M_{1c} = \sqrt{\frac{\gamma + 1}{2\gamma}\left(1 + \frac{\gamma - 1}{2} M_{1h}^2\right)^{\frac{\gamma}{\gamma-1}} + \frac{\gamma - 1}{2\gamma}} \tag{5}$$

where, as previously noted, $M_{1h}^2 = M_{1c}^2 \frac{T_{1c}}{T_{1h}}$. The plot of equations (4) and (5) is the lower (the one closest to the origin) of the two roughly hyperbolic curves of figure 3. In the construction of this dividing line, γ was assumed to be constant and equal to 1.4.

The bubble is characteristically wedge shaped, and the foot of the main shock becomes an oblique shock and reaches down toward the front of the wedge, as indicated in the sketch in figure 3 and as discussed in more detail subsequently. The pressure in the bubble is the previously derived stagnation pressure of the hot flow, and the cold flow behind the oblique shock must have this same pressure; these conditions fix the inclination of the oblique shock. Differentiating between the conditions for which the flow behind the oblique shock (that is, the cold flow over the bubble) is subsonic and the conditions for which it is supersonic is the final step in the classification. The boundary curve is determined as follows: The pressure jump across an oblique shock is

$$\frac{p_{3c}}{p_1} = \frac{2\gamma}{\gamma + 1} M_{1c}^2 \sin^2\epsilon - \frac{\gamma - 1}{\gamma + 1} \tag{6}$$

where ϵ is the inclination of the attached oblique shock. For the case that M_{3c}, the Mach number behind the oblique shock, is one (ref. 9)

$$\sin^2\epsilon = \frac{1}{\gamma M_{1c}^2}\left[\frac{\gamma+1}{4}M_{1c}^2 - \frac{3-\gamma}{4} + \sqrt{(\gamma+1)\left(\frac{9+\gamma}{16} - \frac{3-\gamma}{8}M_{1c}^2 + \frac{\gamma+1}{16}M_{1c}^4\right)}\right] \tag{7}$$

Depending on whether M_{1h} is greater or less than 1, that is, on whether or not a shock occurs in the hot layer, equation (2) or equation (3) gives the rise to stagnation pressure in the hot layer. Equating p_{3c}/p_1 from equation (6), using $\sin^2\epsilon$ from equation (7) with both equations (2) and (3), and using $\gamma = 1.4$ give the third dividing line in figure 2 (the upper roughly hyperbolic curve). The region to the right of the dividing line represents supersonic flow over the bubble. The reason is that with increasing temperature the Mach number M_{1h} in the hot layer is reduced and with it the stagnation pressure p_{oh}. (See eqs. (2) and (3).) As a result, the change in Mach number from the undisturbed flow at M_{1c} to the flow over the bubble at M_{3c} is reduced; in other words, the flow over the bubble becomes more supersonic.

In summary, the interaction patterns may be broadly classified into those with throughgoing hot layers, those with stagnation bubbles and subsonic flow over the bubbles, and those with stagnation bubbles and supersonic flow over the bubbles. Since, for each of these three cases, there are two subtypes, depending on whether or not the hot layer contains a shock, a total of six interaction types have been identified for this case of the normal shock.

THROUGHGOING HOT LAYER

The classification of interaction patterns graphically presented in figure 3 indicates that steady-flow patterns exist with and without shocks in the hot layers. As noted previously, the shock in the supersonic hot layer is the front-running shock familiar to the blast expert. (See fig. 4.) Inasmuch as the interaction is steady, the shock in the hot layer remains at a constant distance from the normal shock moving over the hot layer. Since the pressure across the free boundary of the hot layer is continuous, the shock in the hot layer causes an oblique

shock to extend into the cold flow over the layer. This oblique shock is referred to as the retransmitted shock by writers on blast effects.

When the temperature in the hot layer does not differ much from that in the cold flow, the shock in the hot layer and also the retransmitted oblique shock will not be much weaker than the interacting normal shock. The flow over the hot layer behind the retransmitted shock is thus completely subsonic (fig. 4). Shock patterns of this type, having slightly elevated hot-layer temperatures, have been calculated by Griffith (ref. 6). (Griffith, who permits a continuous temperature variation in the hot layer, also points out that the basic outlines of the interaction pattern show only slight dependence on the temperature profile. This result indicates the feasibility of the present analysis in which a uniform temperature is assumed for the hot layer.)

For hot-layer temperatures differing more from the cold outside flow, the shock in the hot layer is weaker and, as a consequence, the retransmitted shock is also weaker. Thus, a region of supersonic isentropic compression waves has to occur behind the retransmitted shock. (See fig. 5.) When the hot-layer temperature is high enough to require a completely subsonic steady flow in the hot layer for the matching of the cold outside flow, no shock exists, of course, in the hot layer; and thus there is no retransmitted shock. The supersonic isentropic compression waves will coalesce some distance above the hot layer and will cause an oblique shock to extend from that point to a higher point. (See fig. 6.) This shock formed by coalescing of waves may be regarded in a broad sense as a retransmitted shock.

At the intersection of the retransmitted shock, in the restricted and the broad sense, with the interacting normal shock (somewhat deformed), a reflected shock is likely to occur (fig. 5) which has the task of turning the flow partly toward the horizontal. Another part of the turning is accomplished in the subsonic flow behind the reflected-shock region. In a sense, this reflection pattern has some features in common with the triple-shock pattern in a jet exiting against excess pressure shown in figure 39 of reference 4; the Mach reflection would correspond thereby to the interacting normal shock, and the retransmitted oblique shock would correspond to the first shock of this interaction. The considerable difference between these interaction patterns is that the pressure along the free boundary of the jet is constant, whereas the free boundary of the hot layer can support a pressure gradient along it. Whether this pressure gradient prevents the reflected shock from reaching the free boundary is of special interest.

If the reflected shock were to hit the hot layer, its boundary would have a corner, and a stagnation point would occur inside the hot layer. It can be shown, however, that the flow over the hot layer at this

stagnation pressure (of the hot layer) must be subsonic, and this condition prevents the reflected shock from reaching the hot layer. Since this stagnation pressure is the highest pressure in the entire flow field (if it were not, one of the four types with a stagnation bubble would exist), all that is required for proof is to show that the flow over some other hot-layer region lying at lower pressure and higher Mach number is subsonic. The most convenient flow region over the hot layer for the establishing of such proof is the region far downstream where the hot layer approaches the pressure behind the interacting normal shock. Since, however, the flow immediately above the hot layer has a different entropy from that behind the main shock, proof has to be furnished that it is not supersonic at the pressure of the subsonic flow behind the normal shock. The necessity for subsonic flow over this hot-layer region can be inferred by considering the classification of flows as shown in figure 3. The region between the two hyperbolic curves corresponds to stagnation bubbles having subsonic flow over them. Since any point in the throughgoing hot-layer region of figure 3 lies to the left of this region, it must correspond to lower temperature ratios and therefore to more nearly normal retransmitted shocks. Of course, when the temperature of the hot layer is only slightly above that of the cold flow, the retransmitted shock is nearly identical to the interacting normal shock and the flow behind is completely subsonic.

Two appendixes treat the decay of the interaction effects away from the region of largest concentration. Appendix A deals with the upstream decay of a concentrated disturbance in an unlimited steady supersonic flow interacting with a subsonic flow of finite height (the hot layer). These calculations apply to hot layers of sufficiently high temperatures to permit establishment of subsonic flow. However, they probably also approximate the isentropic supersonic compression behind more or less weak retransmitted shocks occurring for lesser hot-layer temperatures. For very small temperature differences, the flow behind the retransmitted shock is subsonic and the analysis of appendix A no longer applies. The calculations made by Griffith (ref. 6) have to be used in this case. Appendix B gives the shape of the interacting shock at large heights where it approaches the normal. Furthermore, this appendix gives the shape of the hot layer downstream of the concentrated-disturbance effects where the flow over the hot layer is subsonic (behind the normal shock).

HOT LAYER WITH STAGNATION BUBBLE

Quasi-Steady Bubble Growth

Strictly speaking, the bubble flow is not quite a steady flow in the same sense that the throughgoing layer was steady. That is, if turbulent mixing effects, such as might serve to limit the size of the

bubble, are neglected, the bubble would simply continue to grow indefinitely as it accumulates more and more stagnation air from the hot layer. The limiting steady-flow case, when the bubble has grown to infinite dimensions, is of little interest.

The case considered herein is that in which the bubble is of finite size, but nevertheless has grown so large that (1) the air velocities within have become mainly too low to produce much variation in pressure throughout most of the bubble and (2) the rate of growth of its linear dimension (which decreases rapidly as the bubble increases in size) has become too small appreciably to affect the pressures in the flow field. Essentially, then, the flow about the bubble is considered, in the main, to be steady at any instant, although the bubble is actually growing. In order to emphasize that the flow pattern is actually slowly changing with time, it is referred to as quasi-steady. The effects of mixing, which can be expected eventually to halt the growth and thereby produce a steady flow, are discussed in a subsequent section.

It is considered that by the time the bubble has grown to several times the hot-layer height the main characteristics of the quasi-steady state already apply because the pressure variations in the bubble vary as the square of the velocity. The airspeeds in the bubble may still differ appreciably from zero (and the height of the bubble is still comparatively reasonable) without causing the internal pressures to deviate very much from stagnation pressure. Accordingly, it is believed that this kind of bubble, in essentially the quasi-steady state, should be observable, in many cases, for a period before it has grown to such size that further growth is limited by turbulent mixing along the boundary.

For an analysis of the shape of the quasi-stagnation bubble and the flow over it, the front and the rear of the bubble are conveniently regarded as separate regions. The flow over the bubble front is assumed to be influenced only by the transition pattern from the undisturbed hot layer to the bubble front and uninfluenced by the eventual downstream adjustment to the high-pressure region behind the normal shock. The flow over the rear of the bubble is assumed to be concerned with this adjustment.

The adjustment of the undisturbed flow to that over the bubble front is as follows: Depending on whether or not the hot layer contains a shock, the flow over the hot layer begins with or without a retransmitted shock. Behind this retransmitted shock the flow experiences supersonic isentropic compression if the flow over the bubble is to be supersonic, or both supersonic and subsonic isentropic compressions for subsonic flow over the bubble. The isentropic supersonic compression waves coalesce to an oblique shock or, if a retransmitted shock already exists, they merely reenforce it. The existence of a subsonic isentropic compression along the hot layer would cause further readjustment of the pressure behind the

oblique shock. If the influence of the rear of the bubble is neglected, a complete adjustment of the pressure behind the oblique shock to the stagnation pressure in the bubble can occur. The flow pattern for the front of the bubble thus consists of a steady oblique shock at Mach number M_{1c} with a pressure jump p_{oh}/p_1 across it. The stagnation region is wedge shaped, the wedge angle corresponding to the oblique shock. (The ambiguity or nonexistence of attached shocks associated with given solid-wedge angles does not apply to the present case where the pressure behind the oblique shock is given.)

The discussion in the preceding paragraph indicates that the bubble grows quasi-steadily within a wedge region. (See fig. 7.) Furthermore, the flow pattern around it experiences nearly geometrically similar growth. When this geometrically similar growth is considered, special attention has to be given to the flow region over the connecting piece between the undisturbed hot layer and the bubble wedge. This connecting flow region, which includes the retransmitted shock with isentropic compression or an isentropic compression alone, produces (in a more or less small strip over the bubble wedge) a flow that has entropy and Mach number different from those behind the oblique shock. The height of this strip remains nearly constant during the bubble growth; consequently, it would violate the requirement of geometrically similar growth if it were not for the fact that it becomes small compared with the bubble size as the steady state is approached. The flow at the entropy and Mach number behind the oblique shock thus represents the effective bubble boundary to the cold outside flow (in the sense of the classification in fig. 3). As the steady state is approached, the length of the connecting region between the undisturbed hot-layer region and the bubble wedge, becomes small also compared with the bubble dimensions. For the pattern growing behind the oblique shock in a wedge-shaped region, the conditions for geometrically similar growth are, of course, satisfied.

The rate of growth of the bubble in the neighborhood of the steady stagnation state can be determined as follows: The mass flow into the quasi-stagnation bubble is a constant quantity determined by conditions in the undisturbed hot-layer region. This constant influx has to equal the rate of growth of the bubble mass. Since the bubble density is almost constant, the rate of growth of the bubble area dL^2/dt is constant. The rate of growth dL/dt is thus inversely proportional to the bubble height L or to the square root of time.

In view of the novel features involved in the bubble formation and growth, possible more exact calculations of the transient-growth effects are of interest. Emphasis is given to the fact that special undisturbed hot-layer shapes exist which are likely to offer further insight into the transient effects with somewhat reduced mathematical effort. For wedge-shaped hot layers, the interaction pattern grows only in size and can be

represented by a single picture. The wedge flows are called pseudo-stationary or conical (in analogy with conical steady flows) in the literature. The usefulness of the wedge-shaped layer has been shown independently in an interesting paper by Jahn (ref. 1) in connection with studies of the refraction patterns of oblique shocks. Especially, note that for a wedge angle approaching zero the interaction patterns approach those of the steady type discussed in this paper. The interaction with hot-layer wedges of various finite wedge angles would offer valuable guidance to the study of transient effects for hot layers approaching constant height. Complete solutions for the interaction of the shock with the hot-layer wedge have not been attained to the present to the author's knowledge, even for the throughgoing hot layer, because the calculations involved are still rather lengthy.

Flow Over Rear of Stagnation Bubble

As the flow moves over the rear of the quasi-steady stagnation bubble, it approaches the wall. When the flow is subsonic, the problem is similar to that arising in cavitation flows. A discussion of some studies in this field is given in reference 5. Moreover, G. Kreisel of the British Admiralty Research Laboratory, England, in 1946 discussed cavitation flows and presented a physical interpretation of the flow over the bubble. Briefly, since, in the flow over the stagnation bubble, the pressure increases with height until it reaches the pressure behind the normal shock where the streamlines are horizontal, the bubble boundary has convex curvature. The bubble cannot meet the wall with a stagnation point since the stagnation pressure of the cold outside flow is larger than that in the hot bubble, whereas the pressure across the free boundary has to be continuous. The possibility that the bubble boundary meets the wall in a concave cusp is ruled out through arguments given by Kreisel. As a result, a so-called reverse or reentrant jet has to move under the hot-layer bubble as sketched in figures 8(a) and 9.

The proofs, such as those given by Kreisel for the necessity of reverse-jet formation, apply directly to potential flow. For flows having variation in total pressures, the establishment of exact requirements for existence of a reverse jet would be more difficult. Total-pressure variations can occur for various reasons: for example, (1) from the entropy variation in a comparatively thin flow strip over the bubble as discussed in the preceding section (2) from the undisturbed hot layer if it had a nonuniform temperature distribution, or (3) in a greater degree from laminar or turbulent mixing along the bubble boundary and boundary-layer effects at the wall. The mixing effects are discussed in the section "Influence of Mixing Inside the Flow and Boundary Layer Near Wall."

For extreme cases of supersonic flow over the bubble, a reverse jet may be avoided if the flow Mach number and the slope at which the boundary

meets the wall were just proper to permit an attached shock at this meeting point. (See fig. 10(a).) An exact analysis is difficult since it would require transonic-flow considerations, the flow behind the normal shock being subsonic. The nonexistence of a reverse jet is the rule rather than the exception when the shock interacting with the hot layer is oblique. This case is discussed in the section "Interaction With Oblique Shocks."

Ideal Flow of Reverse Jet Under Hot Layer

In view of the high pressure behind shock and bubble, the reverse jet will move under the bubble and under the throat region toward the undisturbed hot-layer region, provided that it is not forced to break into the hot layer before it reaches that region. If the reverse jet were forced to turn and break into the hot layer and subsequently envelop pieces of it, these pieces could be carried downstream to the higher pressure region behind the shock. (See fig. 8(b).) The reason for this is that, once enveloped, the pieces are isolated from the undisturbed hot-layer region and the hot-layer throat which transmit the flow to the stagnation bubble. Such an ideal flow break-in would serve, in essence, the same purpose as turbulent mixing, where small fluid regions can be transported to higher pressure.

The problem of break-in of the reverse jet is closely connected with that of the change in shape of the nose of the jet during the motion under the hot layer. The quasi-steady approach is used again for guidance purposes. Through the influence of the high-pressure region behind the bubble, the reverse jet moves under the bubble toward the undisturbed hot-layer region where it takes on the pressure of the undisturbed flow and approaches a constant speed, that is, a constant rate of progress. The reverse jet during its initial motion under the bubble was part of the bubble pattern which approaches a rate of growth inversely proportional to the square root of time. When constant speed at some distance from the bubble is approached, the longitudinal rate of progress of the reverse jet nose has thus divorced itself from the bubble. However, the vertical rate of progress of the jet boundary is still governed by the bubble. The smaller rate of progress of the jet boundary in the vertical direction causes the shape of the jet nose to be flattened rather than bulged out during its progress under the hot layer, a behavior that is certainly opposed to a break-in. To be exact, the height of the reverse jet approaches infinite dimensions as the steady state is approached. Since, as has been pointed out previously, the quasi-steady bubble growth should also apply to bubble heights not too far in excess of the hot-layer height, this flattening of the jet nose will not be restricted to the extreme cases of infinite jet height and complete penetration under the hot layer.

The nature of the rates of progress in the horizontal and vertical directions causes the jet to adopt the shape of a parabola. A break-in of the reverse jet into the hot-layer flow is thus not likely to occur because of ideal flow reasons (a straight wall being assumed) but because of accidental small disturbances causing turbulent mixing along the free jet boundaries. A more concise picture of the transient states of the reverse jet penetration from the beginning of the interaction could be obtained by studying the interaction of a series of hot-layer wedges with angles varying from 90° to 0°.

STABILITY OF IDEAL-FLOW PATTERNS

Since the ideal-flow patterns discussed in the preceding section have free boundaries, it is of interest to consider whether such flows are stable, even when viscosity is disregarded. A general consideration is that the low density in the hot layer has a damping effect on the amplification of small disturbances; also, the centrifugal forces in the cold flow over the bubble boundary have a stabilizing effect.

In general, the flow in the reverse jet will be supersonic because it returns to the upstream undisturbed pressure. The question now arises as to whether two counterflowing supersonic streams (the unlimited cold flow and the reverse cold jet) can exist together, although they are separated by a hot layer. Steady disturbance waves are certainly introduced where the reverse jet penetrates under the bubble and proceeds to adjust its pressure toward the lower value of the undisturbed air. (Compare with the simple case of a supersonic jet issuing into air at rest.) Inasmuch as the jet boundary can give way to disturbances, these will persist far downstream. (See figs. 9 and 10(b).) Accordingly, in order to study the problem, an analysis (appendix C) has been made of the three-layer configuration (cold unlimited flow, hot layers, reverse jet) in which such steady disturbances are assumed. It must be admitted, however, that the problem of existence of three-layer configurations may be of primary concern to the theorist, at least with regard to the present reverse jet, because the assumed deep penetration of the latter is likely to be stopped by mixing effects (except, perhaps, if stability is greatly increased by extreme hot-layer temperatures).

INTERACTION WITH OBLIQUE SHOCKS

With the introduction of oblique incident shocks, the number of possible interaction patterns is very much increased. This variety is already great for the better known interaction with the throughgoing hot layer. (See, for example, ref. 1.) The inclusion of interactions with quasi-stagnation bubbles makes the problems even more involved.

Oblique-Shock Interaction Having Hot Layer With Stagnation Bubble

The division between cases of throughgoing hot layers and hot layers with stagnation bubbles is still given by the criterion that the combined pressure jumps through the incident and the reflected shocks have to match the rise from the undisturbed pressure to the stagnation pressure in the hot layer. No numerical classification of flow patterns for oblique shocks, similar to that presented for normal shocks in figure 3, will be given, however, in view of their great variety; accordingly, only a few interaction types are discussed. When the flow behind the reflected oblique shock is subsonic, the flow over the bubble may be subsonic or supersonic in a similar manner to the interaction with the normal shock. When the flow behind the reflected shock is supersonic, however, the flow over the bubble, which has a stagnation pressure that lies below the pressure behind the reflected shock, has to be always supersonic. Thus, for this case the interaction of the throughgoing hot layer changes directly to the flow types V and VI (fig. 3) with supersonic flow over the bubble.

The requirements for existence of an attached shock where the bubble boundary meets the wall, instead of a reverse jet, are comparatively simple for interactions with oblique shocks inasmuch as the interaction pattern consists of shocks and expansion regions more or less delineated by straight lines. (See fig. 11.) The slope of the front part of the bubble boundary is determined by the oblique shock corresponding to the bubble pressure. The incident shock somewhat deviated by this frontal shock is reflected from the free bubble boundary as an expansion which turns the rear bubble boundary by approximately the same angle as the shock.

If an attached shock is to exist at the end of the bubble, the deviation between the rear bubble boundary and the wall has to be less than the maximum deviation for an oblique shock. (This requirement corresponds closely to that of supersonic flow behind the oblique shock.) The likelihood of attached shocks at the bubble end for supersonic flow behind the reflected oblique shock can be seen from the following approximate reasoning: Assume for the sake of simplicity that the layer is very hot and that the stagnation pressure does not differ much from the undisturbed pressure. As a result, the oblique shock at the beginning of the bubble is weak and the front part of the bubble boundary is nearly horizontal. The incident shock and the reflected expansion turn the bubble boundary approximately twice the deviation through the incident shock (but their combined effect on the Mach number of the flow over the rear of the bubble is small). Since the bubble front is nearly horizontal, the deviation between the bubble end and the horizontal wall at the bubble end must also be about twice the deviation; but the incident and the reflected shocks also turn the flow through approximately twice the

deviation through the incident shock. As a consequence of these about equal deviations, an attached shock, having a supersonic-flow Mach number behind it nearly equal to that behind the reflected shock, is likely to occur at the bubble end.

Oblique Shock Interaction With Throughgoing Hot Layer Having Subsonic Flow

If the temperature of the hot layer is lowered, the interaction with a stagnation bubble (fig. 11) changes to one type of the throughgoing hot layer (fig. 12). A few aspects based on steady-flow concepts, which generally do not appear in the analysis of blast phenomena, is discussed. This interaction has certain aspects in common with results by Tsien (ref. 10) for the interaction of weak oblique shocks with subsonic layers based on small-disturbance calculations. (See also "Subsonic Flow in Hot Layer," appendix A.)

Whether or not an oblique shock interacting with a throughgoing hot layer with subsonic flow can hit the boundary of the layer appears to be also an interesting problem. The reasoning is similar to that for the interaction with a normal shock; however, the result is different. It is assumed that the flow along the hot layer where it approaches the pressure behind the oblique reflected shock is supersonic. If the oblique shock is incident on the hot-layer boundary, a corner is formed with a resulting stagnation point inside the hot layer. The pressure along the hot layer corresponding to stagnation is larger than the pressure behind the reflected shock. (Otherwise, a stagnation bubble would occur.) Thus, depending on the magnitude of the supersonic Mach number along the hot layer behind the reflected shock and of the stagnation pressure in the hot layer, the cold flow over the stagnation point may be supersonic or subsonic. The interacting supersonic oblique shock can thus be incident on the hot layer in contrast to the normal-shock interaction, but need not always be. The small-disturbance approach, of course, cannot bring out this alternative. A more detailed study of such problems would require quantitative classification of the interaction patterns similar to that performed for the normal-shock interaction. High hot-layer temperature favoring supersonic flow along the throughgoing hot layer will also tend to produce a change in flow type similar to that obtained with stagnation bubbles. On the other hand, a comparatively low temperature will produce purely supersonic flow in the hot layer which no longer requires stagnation points where corners occur in the boundary.

The flow pattern having strong shocks in figure 12 differs in other aspects from that with weak shocks in reference 10. As compression waves coalesce to form a shock or as expansion waves impinge on the reflected shock, reflected waves are formed. These reflections constitute new

incident disturbances on the hot layer and produce new interaction patterns. They are, however, so weak that they should not seriously affect the approach to the horizontal of the flow behind the reflected shock. The decay of the interaction effects at more or less large distances from the concentrated effects of shock incidence is discussed in appendix A.

Oblique Shock Interaction With Throughgoing Hot Layer Having Supersonic Flow

As the temperature in the hot layer approaches that of the cold flow, a purely supersonic reflection pattern occurs in the hot layer. (See fig. 13.) The patterns have features in common with those for a supersonic free jet embedded in a supersonic stream. (See the analysis in refs. 11 and 12 and in "Supersonic Flow in Hot Layer" of appendix A of this paper.) Briefly, weak shocks are reflected as shocks or expansions according to whether or not the impedance $M^2/\sqrt{M^2 - 1}$ of the hot layer is larger or smaller than that of the cold flow. The word "impedance" is used in analogy with the acoustic term (ref. 13). For strong shocks the impedance is of a more complicated nature. (See ref. 1.) For equal impedances of the two flows, the incident shock is refracted into the hot layer without reflection (fig. 13(b)) while inclined at the complementary angle. The following proof of this fact is given: Since $\frac{1}{M} = \sin \alpha$,

$$\frac{\sqrt{M^2 - 1}}{M^2} = \frac{\sin 2\alpha}{2}$$

Also, $\sin 2\alpha = \sin(\pi - 2\alpha)$; therefore α or $\frac{\pi}{2} - \alpha$ corresponds to the same value of the impedance. For equal impedance, of course, the additional trivial solution of equal temperatures and Mach numbers in the hot and cold flows also occur.

A great variety of intermediate interaction patterns exist between those with purely subsonic flow in the hot layer (for example, fig. 12) and those with purely supersonic flow. (See fig. 13.) These intermediate interaction patterns have received special attention in blast studies. In these studies an additional classification is introduced into regular and irregular refraction patterns in analogy with acoustic and optical usage. (See, for example, ref. 1.) A regular refraction pattern is characterized by the fact that it can be determined completely by matching conditions at the point of incidence of the shock on the hot-layer boundary. For irregular refractions subsonic-flow regions occur which no longer permit matching of the pattern at a single point; thus,

transonic-flow considerations are frequently involved. The normal-shock interactions previously discussed in this paper are, of course, of this irregular type. In the studies of irregular refractions the formation of the front-running shock (which is herein the shock in the hot layer) is studied in some detail. A feature not covered so far in this paper is the formation of the Mach stems. Since Mach stems are formed predominantly for interactions with spherical shocks, they are discussed in this connection.

INTERACTIONS WITH MACH STEMS FOR OBLIQUE AND SPHERICAL SHOCKS

General Remarks

If an oblique shock interacting with a wall has an angle of incidence larger than a certain critical value, an oblique reflected shock which turns the flow back parallel to the wall can no longer be found. Dimensional reasoning indicates that for the existence of a Mach stem, that is, a nearly normal shock of finite dimension, some other characteristic finite dimension has to exist for the flow. For example, the distance from a corner in the wall where an interaction begins may serve as the characteristic dimension. A finite length is also introduced without deformation of the wall, but rather by deformation of the plane incident oblique shock into a curved one, in particular, into a spherical shock. Such shocks have a finite dimension at any given time and have their own beginning under the explosion center. The presence of a hot layer with finite height or with a finite wedge angle also introduces a dimension and thus makes the occurrence of a Mach stem possible. Of course, the presence of any finite height is not enough for the occurrence of a Mach stem. Since the pressure behind the nearly normal Mach stem must be higher than the pressure behind the oblique reflected shock, an expansion region has to exist in the flow behind the Mach stem. This region may be supersonic or subsonic or a combination of both. (For Mach stems in, for example, steady jet flows of finite height, see figs. 39 and 76 of ref. 4.)

An intermediate pattern between cases of purely subsonic and purely supersonic flow in the hot layer (figs. 12 and 13) can be imagined, a Mach stem occurring next to the wall in the hot layer (fig. 14). The existence of interaction patterns with Mach stems over the hot layer due to an oblique incident shock has been observed in the experiments of reference 1, where plausibility considerations are also presented in support of the patterns. An exact analysis of the Mach stem patterns would be difficult even for the present steady-flow interaction with a layer of constant height, since the deformations of the hot-layer boundary presents an added difficulty.

In almost all blast phenomena the occurrence of a Mach stem over the hot layer is primarily due to the fact that the interacting shock is a spherical shock instead of a plane oblique shock. As previously noted, such a curved shock has a finite dimension of its own and thus does not need the hot layer to introduce a characteristic dimension. In the present blast case the interacting shocks are spherical and the Mach stem will be partly due to the finite extent of the spherical shock and the finite height of the hot layer. A composite picture of these effects is shown in figure 15 which shows results of experiments with cylindrical shocks by Varwig and Zemel at the Naval Ordnance Laboratory in 1955. Cylindrical shocks have many features in common with the spherical shocks occurring in blasts but permit simple analysis and experimental observation since their motion occurs in a plane. In the subsequent section the Mach stem formation observed by Varwig and Zemal is discussed in somewhat greater detail.

Quasi-Steady Interactions With Mach Stems for Spherical or Cylindrical Shocks

A curved shock having a finite dimension does not need the finite hot-layer height to produce a Mach stem. The basic nature of the curvature influence can thus be brought out for interaction of the shock with the wall alone; the actual Mach stem is, of course, a composite of shock-curvature and hot-layer influence. Since the mathematical analysis of the transient interaction with spherical or cylindrical shocks is already very involved when the shocks are weak (ref. 3), it is again desirable to look to the cases of quasi-steady flow for guidance. A steady state is approached for the interaction of a spherical or a cylindrical shock with a wall when the changes in incidence and shock strength as the shock moves along the wall are small compared with the distance traveled along the wall; in other words, when the radial distance to the explosion center is far from the section of the wall being considered, the shock strength, incidence angle at the wall, and curvature change so slowly that at any instant the flow pattern may be taken as quasi-steady. An exactly steady state, however, cannot be of interest for the present discussion because it would imply an infinite shock radius for which there could be no Mach stem.

The curvature of the incident shock is produced by quasi-steady supersonic expansion waves behind the shock (fig. 15). Note that spherical or cylindrical shocks produce expansion regions behind them as their surface increases; a slow increase produces a quasi-steady supersonic expansion region. (This supersonic expansion, in turn, influences the reflected shock so that it can bring about the pressure reduction behind the Mach stem which is necessary for its finite height.) The effect of the Mach stem on the hot layer is similar to that of a normal shock shown

in figures 4 and 5. Accordingly, near the hot-layer boundary the Mach stem is diffused into isentropic compression waves. The flow behind the diffused compression as well as behind the reflected shock is assumed herein to be completely subsonic; the region behind the reflected shock could also, of course, be supersonic without violating the broad principles in the present discussion. The deformation of the hot layer can also produce expansions which, together with the expansions responsible for the curvature of the incident shock, yield the dimensions of the Mach stem.

A tentative ideal-flow interaction of a cylindrical shock and a hot layer with bubble formation is given in figure 16. For reasons discussed previously, this interaction is, of course, only an approximate composite of the interaction patterns with oblique shocks of various incidences.

INFLUENCE OF MIXING INSIDE THE FLOW AND BOUNDARY LAYER NEAR WALL

Experimental studies of interactions with throughgoing hot layers show that the mixing along the boundary has only small influence on the ideal-flow patterns. This fact can be explained as follows: The laminar or turbulent mixing along the free hot-layer boundary is essentially due to the difference in velocities along this boundary created through disturbance of the hot layer by the incident shock. The importance of the mixing effects compared with the potential-flow effects can be estimated through a Reynolds number $\rho \Delta U l/\mu$. The length l is the distance of that section of the hot-layer boundary along which the effects of steady ideal flow cause the dominant deviations from the horizontal. Dimensional reasoning and small-disturbance calculations in appendixes A and B indicate that for the throughgoing hot layer this distance is of the order of the hot-layer height upstream and downstream of the incident shock. For interactions with bubble formation the length l represents the characteristic linear bubble dimension. (Mixing extends, of course, infinitely far downstream of the incident shock, but for the present purposes its effects on the region of dominant deformation of the ideal-flow pattern are of primary concern.) The velocity factor ΔU is the average velocity difference along the length l. The density ρ and the viscosity μ are averaged values of the hot and cold flows. For throughgoing hot layers of comparatively small height, l is small and thus the Reynolds number is small; therefore, the ideal-flow pattern should not be seriously affected by mixing. For interactions of hot layers of small height with bubble formation, l is larger; however, these interactions also correspond to higher temperatures. As a consequence, ρ is reduced, μ is increased, and each of these changes reduces the Reynolds number and thus the effect of mixing. In accordance with these expectations, the interferograms of interactions with hot layers of small height (refs. 2 and 6)

match the present ideal-flow approximations fairly closely. Note especially that the criterion of shock strength and hot-layer temperature found to be necessary for bubble formation (ref. 9) is not far removed from that given in the present classification of flow patterns.

For hot layers of larger height than those produced in the laboratory, the Reynolds number becomes larger; thus, the mixing effects should become more important for corresponding states of development of the interaction. In view of the more important mixing effects, the bubble growth for layers of large height may deviate to some extent from the quasi-steady law. The stronger influence of mixing, however, does not rule out the bubble formation and formation of reverse jets as shown subsequently.

The mixing reduces the bubble growth by entraining and removing mass from the bubble. A steady-flow pattern with mixing is ultimately attained (figs. 17 and 18) when this loss in mass equals that supplied by the hot-layer flow into the bubble. It has certain aspects in common with the pattern of the separation bubble because of the reattachment of steady boundary-layer flows. Some important differences are discussed subsequently.

The steady mixing-flow pattern, in view of its permanence, is independent of the manner in which it is built up. A dividing streamline can be defined between the circulatory flow inside the bubble and the flow over it along which the turbulent mass exchange of hot and cold air is in the mean zero. The circulatory flow, having in the mean no mass additon, is maintained by momentum and energy exchange with the flow around the bubble. Part of the circulatory flow has a direction opposed to the cold outside flow. This reverse flow which contains in the mean no mass addition from the outside flow has to be carefully distinguished from the ideal-flow reverse jet which contains mass from the outside flow.

Important differences exist between the present separation bubble and the better known separation bubble occurring in steady boundary-layer flow over wings and in diffusers. The present separation bubble is part of the steady flow relative to the moving shock, whereas in the usual boundary-layer case the flow is steady with respect to the wall. In the steady-flow system moving with the shock, the wall "pulls" the fluid along. Such behavior is in direct contrast to the customary boundary layer which is retarded by the wall; it is, however, related to the boundary layer in shock tubes. (For example, see refs. 14, 15, and 16.) In other words, because of the high speed of the wall (in the steady flow relative to the moving shock), the flow regions near the wall will have a higher total pressure than those away from the wall. Thus, the flow will not separate from the wall as is the case with usual boundary layers; rather, it will "separate" from the inside of the hot layer and reattach itself again inside, further downstream. Since momentum and energy can be imparted now from two sides, from the moving wall in addition to the cold flow over the hot layer, the separation bubble will be divided into two

circulatory flows. The establishment of a criterion to distinguish between mixing patterns of the throughgoing hot layer and those with separation bubble is, of course, far more difficult than that for ideal flow. Since mixing increases the total pressure of the hot air near the boundary, it will require higher temperature ratios for bubble formation than ideal flow does.

A more detailed discussion of figures 17 and 18 may be useful. A mean dividing streamline separates the bubble from the flow around it. Since a double circulation occurs inside the separation bubble, it is also divided by a streamline. Another streamline divides the cold outside region from the flow around the separation bubble; the wall is the dividing streamline of the boundary-layer flow. The wavy lines indicate approximate boundaries along which the spreading of the mixing regions and the boundary-layer regions occur. The heavily drawn spiral is a reminder of the fact that the separation bubble of the hot layer is cooled by the intermixing of the cold outside flow. Since the mixed flow permits transverse Mach number gradients, it can reflect oblique shocks as compressions as well as expansions (see fig. 18) in contrast to the ideal-flow interaction in figure 11. Figure 16.49 in reference 17 was used as a guide for sketching the outside flow in figure 18.

Finally, it may be of interest to note that such steady separation bubbles with double-circulation patterns would appear also to be possible for the interaction of shocks with certain turbulent wake regions behind bodies or combustion zones, which also have high total pressures near their boundaries.

CONCLUSIONS

The following conclusions have been reached from a study of the interaction between hot layers extended along a wall and normal or oblique shocks moving over them:

1. For normal and oblique shocks interacting with a hot layer of constant height, the transient-interaction effects decay and the interaction can be considered to be steady relative to the moving shock.

2. For the steady flow relative to the normal shock, a classification into six types of interaction patterns is possible. The main division is based on the fact that for very high temperatures the stagnation pressure of the hot-layer flow lies below the pressure behind the normal shock. As a consequence, the hot-layer flow can no longer approach this high-pressure region as it does for lower temperatures and has to accumulate in a bubble-like region. The interaction pattern with a bubble may be divided again into two cases, depending on whether the flow in the hot layer is supersonic (contains a shock) or is subsonic.

3. Useful information about the bubble growth is obtained from quasi-steady-flow considerations. It is shown that the quasi-steady growth occurs in a wedge-shaped region. When the flow over the bubble is subsonic, it may divide as it moves over the rear of the bubble toward the wall and force a jet of cold air to move under the bubble. A supersonic flow over the bubble can meet the wall with a shock.

4. Under the influence of mixing, the bubble stops growing and becomes part of a steady separated flow pattern. The separation bubble differs importantly from that occurring in steady boundary-layer flows because it is bound to the moving shock. Consequently, momentum is not only imparted by the cold flow but also by the wall, which pulls the flow along rather than retarding it. The separation bubble will contain two circulatory flows instead of one. The pattern of flow separation has aspects in common with those produced by shocks with wakes behind bodies or combustion zones where momentum is imparted also from both boundaries.

5. For interaction with an oblique shock the hot-layer flow accumulates in a bubble when its stagnation pressure can no longer match the pressure behind the combined incident and reflected shocks. The flow over the bubble is predominantly supersonic and, in most cases, meets the wall with a shock; thus, a jet of cold air need not move under the bubble.

6. As in the interaction with a normal shock, the alternatives of hot-layer flows with and without shocks exist. In contrast, the hot-layer flow can now contain oblique shocks with a great variety of reflection patterns. Some of these patterns are very closely related to those encountered for supersonic jets embedded in supersonic streams.

7. The interaction of spherical or cylindrical shocks with hot layers can be treated in some cases with a quasi-steady approach. This approach also yields some information concerning the nature of triple-shock patterns with Mach stems over the hot layer.

Langley Aeronautical Laboratory,
National Advisory Committee for Aeronautics,
Langley Field, Va., February 26, 1957.

APPENDIX A

DECAY OF STEADY INTERACTION EFFECTS OF UNLIMITED SUPERSONIC FLOW WITH HOT LAYER OF FINITE HEIGHT

Subsonic Flow in Hot Layer

Decay effect for interaction.- The dominant effects of the more or less concentrated disturbance produced by the incident shock will decay to vanishingly small values at sufficient distances upstream and downstream of the shock. The final or asymptotic decay of these disturbance effects can be treated by a small-disturbance approach, regardless of whether the incident shock is strong or weak. These decay calculations in this appendix apply only to regions where the flow over the hot layer is supersonic; thus, they apply to the hot-layer regions downstream as well as upstream of the incident shock if the flow downstream of the latter is supersonic. This is the case for many interactions of oblique shocks; however, for a normal shock interacting with a subsonic hot layer only the flow upstream of the shock is supersonic. The asymptotic decay for the hot-layer regions under the subsonic flow behind the normal shock is analyzed in appendix B. The asymptotic decay applies, of course, only where no new disturbance occurs, such as a shock in the hot layer; that is, it applies to isentropic-flow interactions. (See fig. 6.) For comparatively weak shocks in the hot layer, however, the present asymptotic decay effects should apply to the isentropic region upstream of the incident shock and behind the shock in the hot layer.

The small-disturbance approach was used in reference 10 to calculate the complete-flow pattern even in the neighborhood of the (oblique) incident shock which was assumed to be of small strength; the results were conveniently developed with the aid of Fourier integral transforms. For the present case, where only the asymptotic decay of (possibly large) disturbances is treated, it is more convenient to study the disturbance effects in terms of elementary functions, similar to the method described in reference 8 for the flow over a wavy wall. However, the method is used herein for the decay of disturbances. The decay upstream of the concentrated disturbances is treated first.

The small-disturbance potential of the supersonic flow above the hot layer of height y_{1h}, in terms of the elementary decay function, is

$$\phi_c = u_1 A e^{\frac{1}{s}\left(x - y\sqrt{M_{1c}^2 - 1}\right)} \qquad \left(y_{1h} < y < \infty\right) \qquad (A1)$$

Since the supersonic flow over the hot layer is unlimited, only one family of Mach waves is required. The Mach waves designated in equation (A1) correspond to a flow in the positive x-direction. From a broader viewpoint, the selection of only one group of Mach waves has the purpose of satisfying the boundary conditions of the cold supersonic flow at infinite height over the hot layer. When the problem is solved in terms of elementary functions, the problem of satisfying the boundary conditions at the concentrated disturbance does not arise. The concentrated disturbance has to be accounted for by superimposing a variety of elementary disturbances; this problem, however, is not treated herein. Since the flow in the hot layer is subsonic, the factor representing the y-component of the small-disturbance potential must be represented by an elementary function of the following sinusoidal form:

$$\phi_h = u_1 A^* e^{x/s} \cos\left(\frac{y}{s}\sqrt{1 - M_{1h}^2}\right) \qquad \left(0 < y < y_{1h}\right) \tag{A2}$$

The term $\cos(\ )$ in equation (A2) is chosen in order to satisfy the boundary condition that the normal velocity $\partial\phi/\partial y$ be zero at the wall. The quantity s is the decay modulus of the exponential decay and is representative of the distance required for the decay of the essential part of the disturbance effects. Positive values of s correspond to disturbances decaying in the upstream direction, that is, in the negative x-direction; whereas negative values of s correspond to downstream decay. The quantity s in equations (A1) and (A2) is the unknown which is to be determined by matching slopes and pressures of the hot and cold flows at the hot-layer boundary.

The slopes $(\partial\phi/\partial y)\Big/u_1$ of the streamlines in the cold outside flow and in the hot layer are, respectively,

$$\frac{1}{u_1}\frac{\partial\phi_c}{\partial y} = -A\,\frac{1}{s}\sqrt{M_{1c}^2 - 1}\; e^{\frac{x}{s}} e^{-\frac{y}{s}\sqrt{M_{1c}^2-1}} \tag{A3}$$

and

$$\frac{1}{u_1}\frac{\partial\phi_h}{\partial y} = -A^*\,\frac{1}{s}\sqrt{1 - M_{1h}^2}\; e^{x/s} \sin\left(\frac{y}{s}\sqrt{1 - M_{1h}^2}\right) \tag{A4}$$

The respective pressure increments relative to the undisturbed pressure,

$$\frac{\Delta p}{p_1} = \frac{\gamma M_1^2 \Delta u}{u_1} = \frac{\gamma M_1^2 \left(\frac{\partial \phi}{\partial x}\right)}{u_1}$$

are given as

$$\frac{\gamma M_{1c}^2}{u_1} \frac{\partial \phi_c}{\partial x} = A\gamma M_{1c}^2 \frac{1}{s} e^{\frac{x}{s}} e^{-\frac{y}{s}\sqrt{M_{1c}^2-1}} \tag{A5}$$

and

$$\frac{\gamma M_{1h}^2}{u_1} \frac{\partial \phi_h}{\partial x} = A^*\gamma M_{1h}^2 \frac{1}{s} e^{x/s} \cos\left(\frac{y}{s}\sqrt{1 - M_{1h}^2}\right) \tag{A6}$$

Equating the slopes and pressures at the hot-layer boundary y_{1h} yields, respectively, the following two ratios of the coefficients:

$$\frac{A^*}{A} = \frac{\sqrt{M_{1c}^2 - 1}}{\sqrt{1 - M_{1h}^2}} \frac{e^{-\frac{y_{1h}}{s}\sqrt{M_{1c}^2-1}}}{\sin\left(\frac{y_{1h}}{s}\sqrt{1 - M_{1h}^2}\right)}$$

and

$$\frac{A^*}{A} = \frac{M_{1c}^2}{M_{1h}^2} \frac{e^{-\frac{y_{1h}}{s}\sqrt{M_{1c}^2-1}}}{\cos\left(\frac{y_{1h}}{s}\sqrt{1 - M_{1h}^2}\right)}$$

Equating the two ratios and solving for the decay modulus s at the hot-layer boundary give

$$s = \frac{y_{1h}\sqrt{1 - M_{1h}^2}}{\tan^{-1}\left(\frac{M_{1h}^2}{M_{1c}^2} \frac{\sqrt{M_{1c}^2 - 1}}{\sqrt{1 - M_{1h}^2}}\right) \pm n\pi} \tag{A7}$$

The appearance of the term $\tan^{-1}(\ )$ in equation (A7) indicates that the values for the decay modulus s are multivalued, and each corresponds to an elementary solution. The multivaluedness introduces negative as well as positive values, which describe the upstream and the downstream decay, respectively. Since adding and subtracting $n\pi$ from a fixed value of $\tan^{-1}(\ )$ gives different absolute values of s, the upstream and downstream decays are asymmetric.

It still remains to single out those elementary solutions which represent the asymptotic decay. The asymptotic decay corresponds to the solutions with the largest positive or negative values of s representing upstream or downstream decay, respectively. The largest positive s, or the smallest denominator in equation (A7), corresponds to $n = 0$. The largest negative value of s, however, occurs for $n = 1$. The values of the asymptotic decay modulus depend, of course, on the hot-layer height, the Mach number of the supersonic flow over the hot layer M_{1c}, and the Mach number of the subsonic flow in the hot layer M_{1h}.

Comparison with Fourier integral method.- The results obtained by the Fourier integral method in reference 10 can be reduced to the present results which are in terms of elementary functions. The comparison will be made first for positive values of s corresponding to upstream decay. In reference 10, the decay modulus is not given directly, but the deviation η of the interface from the horizontal (eq. (44) with $\xi < 0$) and the slope $d\eta/dx$ (eq. (43) with $\xi < 0$) are found. The decay modulus s is equivalent to the subtangent of the decay, and is thus obtained by dividing η by the slope $d\eta/dx$; in the present symbols $s = \dfrac{\Delta y}{d\Delta y/dx}$. (See fig. 5.) Note that the expressions for η and $d\eta/dx$ in reference 10 are sums over the elementary functions for various values of n. For a comparison with the present results in terms of elementary functions, the values of s are thus obtained by division of the expressions under the summation signs rather than the sums. Substituting the present values y_{1h} and M_{1h} for the thickness b and the Mach number M_2 in reference 10 gives

$$s = \frac{\Delta y}{d\Delta y/dx} = \frac{2y_{1h}\sqrt{1 - M_{1h}^2}}{\pi\left(2n + 1 - \frac{\theta}{\pi}\right)} = \frac{y_{1h}\sqrt{1 - M_{1h}^2}}{\frac{\pi}{2} - \frac{\theta}{2} + n\pi}$$

The quantity $\theta/2$ is expressed by equation (24) of reference 10 as

$$\frac{\theta}{2} = \cos^{-1} \frac{\frac{M_{1h}^2}{M_{1c}^2}}{\sqrt{\frac{M_{1h}^4}{M_{1c}^4} + \frac{1 - M_{1h}^2}{M_{1c}^2 - 1}}} = \cos^{-1} \frac{\frac{M_{1h}^2}{M_{1c}^2} \frac{\sqrt{M_{1c}^2 - 1}}{\sqrt{1 - M_{1h}^2}}}{\sqrt{\left(\frac{M_{1h}^2}{M_{1c}^2} \frac{\sqrt{M_{1c}^2 - 1}}{\sqrt{1 - M_{1h}^2}}\right)^2 + 1}}$$

$$= \cos^{-1} \frac{b}{\sqrt{b^2 + 1}}$$

where

$$b = \frac{M_{1h}^2}{M_{1c}^2} \frac{\sqrt{M_{1c}^2 - 1}}{\sqrt{1 - M_{1h}^2}}$$

Since $\frac{\pi}{2} - \frac{\theta}{2} = \frac{\pi}{2} - \cos^{-1} \frac{b}{\sqrt{b^2 + 1}} = \sin^{-1} \frac{b}{\sqrt{b^2 + 1}} = \tan^{-1} b$, the decay modulus s may be written in the form

$$s = \frac{y_{1h}\sqrt{1 - M_{1h}^2}}{\tan^{-1} \frac{M_{1h}^2\sqrt{M_{1c}^2 - 1}}{M_{1c}^2\sqrt{1 - M_{1h}^2}} + n\pi} \tag{A8}$$

Equation (A8) is the same as that in equation (A7) with a positive $n\pi$. For a comparison of equation (A8) with equation (A7) with a negative $n\pi$, η from equation (44) with $\xi > 0$ (ref. 10) has to be divided by $d\eta/dx$ from equation (43) with $\xi > 0$ (ref. 10). This division results (in present terminology) in

$$s = -\frac{y_{1h}\sqrt{1 - M_{1h}^2}}{\frac{\pi}{2} + \frac{\theta}{2} + n\pi} + (\text{Sum of constants}) \frac{1}{e^{-\left[2n+1+(\theta/\pi)\right]|\xi|}} \tag{A9}$$

The last term which is introduced through equation (44) for the height of the hot layer indicates that, far downstream from the shock, the hot layer approaches a greater constant height than it has in the undisturbed region. Specifically, the approach of the denominator to zero as $\xi \to \infty$ means that $s \to \infty$, that is, an approach of the hot layer to zero boundary slope or constant height. The first term represents a perturbation of the downstream hot-layer region of greater height; this term is to be identified with equation (A7) by using a negative $n\pi$ in the denominator. In order to show this identity the denominator of equation (A7) is written in the form $\pi/2 - \theta/2 - n\pi$ and the minus sign of equation (A9) is taken into the denominator; the result is $-\pi/2 - \theta/2 - n\pi = \pi/2 - \theta/2 - (n + 1)\pi$. The two denominators are thus identical if n is replaced by $n - 1$.

Decay with one-dimensional channel-flow approximation in hot layer.- Since in the classification of interaction types use was made of channel-flow approximation, it is of interest to apply the small-disturbance approach also to this case. The simple calculations also represent a further check of the previous calculations. The relative pressure rise in the subsonic hot layer is (ref. 8)

$$\frac{\Delta p}{p_1} = -\gamma M_{1h}^2 \frac{\Delta u}{u_1} = \frac{\gamma M_{1h}^2}{1 - M_{1h}^2} \frac{\Delta y}{y_{1h}} \tag{A10}$$

The relative pressure rise for the unlimited supersonic flow over the hot layer is

$$\frac{\Delta p}{p_1} = \frac{\gamma M_{1c}^2}{\sqrt{M_{1c}^2 - 1}} \frac{d\Delta y}{dx} \tag{A11}$$

The decay modulus s is

$$s = \frac{\Delta y}{d\Delta y/dx} = \frac{M_{1c}^2\left(1 - M_{1h}^2\right)}{M_{1h}^2\sqrt{M_{1c}^2 - 1}} y_{1h} \tag{A12}$$

Equation (A7) with $n = 0$ in the denominator reduces to equation (A12) based on the channel-flow approximation in the hot layer for small values of $M_{1h}^2\sqrt{M_{1c}^2 - 1}\Big/M_{1c}^2\sqrt{1 - M_{1h}^2}$, where $\tan^{-1}( )$ can be replaced by its argument. Note that the decay modulus s in equation (A12) can take on only positive values in contrast to s in

equation (A7) which can be positive or negative. The use of the channel-flow approximation in combination with the present small-disturbance approach would thus yield partly misleading results. For the classification of flow patterns given in the body of the report based on matching the complete pressure rise in the hot layer with that through the shock (or shocks) in the cold outer flow, however, the channel-flow approximation is very useful.

Supersonic Flow in Hot Layer

The present small-disturbance calculations apply to reflection patterns of the type shown in figure 13. The following small-disturbance potential of the unlimited cold supersonic flow is the same as that given in equation (A1):

$$\phi_c = u_1 B e^{\frac{1}{s}\left(x - y\sqrt{M_{1c}^2 - 1}\right)} \qquad \left(y_{1h} < y < \infty\right) \tag{A13}$$

The supersonic flow in the hot layer of finite height includes both families of Mach waves and thus has to include the sum of two exponentials, with both $\left(x + y\sqrt{M_{1h}^2 - 1}\right)$ and $\left(x - y\sqrt{M_{1h}^2 - 1}\right)$ as exponents. The boundary condition at the wall requires the sum of the two terms to be of the form

$$\phi_h = u_1 B^* e^{x/s} \cosh\left(\frac{y}{s}\sqrt{M_{1h}^2 - 1}\right) \qquad \left(0 < y < y_{1h}\right) \tag{A14}$$

Solving again for the decay modulus s by matching the slopes and pressures at the hot-layer boundary results in

$$s = -\frac{y_{1h}\sqrt{M_{1h}^2 - 1}}{\tanh^{-1}\dfrac{M_{1h}^2\sqrt{M_{1c}^2 - 1}}{M_{1c}^2\sqrt{M_{1h}^2 - 1}} \pm in\pi} \tag{A15}$$

and

$$s = -\frac{y_{1h}\sqrt{M_{1h}^2 - 1}}{\tanh^{-1}\dfrac{M_{1c}^2\sqrt{M_{1h}^2 - 1}}{M_{1h}^2\sqrt{M_{1c}^2 - 1}} \pm i\left(n + \frac{1}{2}\right)\pi} \tag{A16}$$

where equations (A15) and (A16) hold for values of $\frac{M_{1c}^2\sqrt{M_{1h}^2 - 1}}{M_{1h}^2\sqrt{M_{1c}^2 - 1}}$ smaller or larger than unity, respectively; for simplicity this ratio is designated by K. The basic reason for the difference in form is that the function $\tanh^{-1}(K)$ has no real values for $K > 1$, whereas for $K < 1$ it has both real and complex values. The real values for $K < 1$ are obtained by setting $n = 0$ in equation (A15). Letting $k = \tanh^{-1}(K) \pm in\pi$ for $K < 1$ gives

$$k = \frac{1}{2} \log_e \frac{1 + K}{1 - K} \pm in\pi$$

$$= \frac{1}{2} \log_e - \left(\frac{1 + \frac{1}{K}}{1 + \frac{1}{K}} \right) \pm in\pi$$

and

$$k = \tanh^{-1} \frac{1}{K} \pm i\left(n + \frac{1}{2}\right)\pi$$

Equation (A15) is of the same structure as (A7) except that $\tanh^{-1}(\ )$ appears in the denominator instead of $\tan^{-1}(\ )$. Note that the $\tanh^{-1}(\ )$ has its multivaluedness in the complex domain. Equations (A15) and (A16) also indicate, as expected, that for supersonic flow in the hot layer only negative decay moduli s can exist; these moduli correspond to a downstream decay. Equations (A15) and (A16) could have been obtained directly from equation (A7) by formal manipulation. For $M_{1h} > 1$, that is, supersonic flow in the hot layer, and for $\tanh^{-1}(\ ) = i \tan^{-1} i(\ )$, equation (A7) is transformed into equation (A15) or (A16).

The complex values of s correspond to a complex exponential decay function of the form $Ae^{x/s}$ where $\frac{1}{s} = \frac{1}{\sigma} \pm i\omega$. The real exponential decay modulus is thus σ and the wavelength λ is $2\pi/\omega$. The elementary functions for the interaction of the unlimited supersonic stream with a finite supersonic hot layer are thus generally exponentially decaying harmonic oscillations. The only exception is the case in which $n = 0$ in equation (A15) when s is real, and the exponential decay is nonoscillatory. Before discussing the superposition of these elementary disturbances to concentrated Mach wave disturbances, certain physical

features of the interaction are examined with the aid of the elementary functions. The values of σ and λ corresponding to equation (A15) for $K < 1$ are

$$\left.\begin{aligned} \sigma &= \frac{1}{R\left(\frac{1}{s}\right)} = -\frac{y_{1h}\sqrt{M_{1h}^2 - 1}}{\tanh^{-1}K} \\ \lambda &= \frac{2\pi}{I\left(\frac{1}{s}\right)} = \frac{2y_{1h}\sqrt{M_{1h}^2 - 1}}{n} \end{aligned}\right\} \tag{A17}$$

and those corresponding to equation (A16) for $K > 1$ are

$$\left.\begin{aligned} \sigma &= \frac{1}{R\left(\frac{1}{s}\right)} = -\frac{y_{1h}\sqrt{M_{1h}^2 - 1}}{\tanh^{-1}\frac{1}{K}} \\ \lambda &= \frac{2\pi}{I\left(\frac{1}{s}\right)} = \frac{2y_{1h}\sqrt{M_{1h}^2 - 1}}{n + \frac{1}{2}} \end{aligned}\right\} \tag{A18}$$

The different behavior of the complex decay for $K < 1$ and $K > 1$, appearing in essence in the wavelengths λ in equations (A17) and (A18), is now given a physical interpretation. For that purpose, $\sqrt{M_{1h}^2 - 1}$ is expressed as $\cot \alpha$, where α is the Mach angle. The wavelength λ corresponding to equation (A17) for $K < 1$ becomes

$$\lambda = \frac{2y_{1h} \cot \alpha}{n}$$

whereas λ corresponding to equation (A18) for $K > 1$ becomes

$$\lambda = \frac{2y_{1h} \cot \alpha}{n + \frac{1}{2}}$$

The significance of these different expressions for λ is best shown by using definite values for the integers n. For $n = 1$, $\lambda = 2y_{1h} \cot \alpha$ with $K < 1$ whereas for $K > 1$, $\lambda = \frac{4}{3} y_{1h} \cot \alpha$. These expressions

are best illustrated by representative sketches. The wavelength $\lambda = 2y_{1h} \cot \alpha$ shows a harmonic disturbance that is repeated as follows:

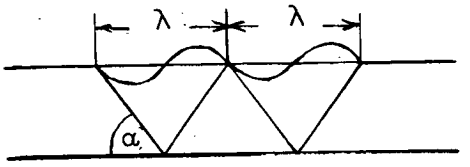

$K < 1$

The wavelength $\lambda = \frac{4}{3} y_{1h} \cot \alpha$ shows a different repetition

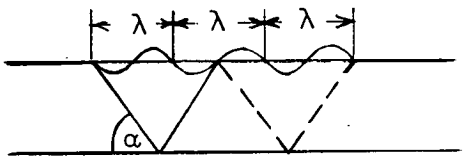

$K > 1$

The sketches show that for $K < 1$, a harmonic disturbance is repeated in its original form after reflection of the first Mach wave has hit the hot-layer boundary. For $K > 1$ the opposite, that is, the negative of the initial disturbance, is reflected from the hot-layer boundary. For example, for $K < 1$ compressions are reflected as compressions whereas for $K > 1$ compressions are reflected as expansions.

Furthermore, a real decay modulus exists only for $n = 0$ with $K < 1$; the nonoscillatory type of exponential decay is the exception for this purely supersonic interaction. Note also that the impedance $M^2/\sqrt{M^2 - 1}$ has a minimum at $M = \sqrt{2}$; this fact may be useful in determining whether K is larger or smaller than one. (For example, if M_{1h} is close to one but M_{1c} is close to $\sqrt{2}$, K will be larger than one.)

Consider the values of σ and λ for the special cases that $K \to 1$ and $M_{1h} \to 1$. As $K \to 1$, $\sigma \to 0$ while the wavelength λ remains finite. As $M_{1h} \to 1$, $K \to \infty$ or $1/K \to 0$ and equation (A18) applies. In the case that $M_{1h} \to 1$ from the supersonic side, $\sigma \to y_{1h}\sqrt{M_{1c}^2 - 1}/M_{1c}^2$ whereas $\lambda \to 0$. This result is of importance to the analysis in appendix C. In contrast, when $M_{1h} \to 1$ from the subsonic side (eq. (A7)), the decay modulus becomes zero. The discontinuity of the decay modulus at $M_{1h} = 1$

is due to linearization of the flow equations. For $K \to 1$ in equations (A17) and (A18) no discontinuity in σ occurs because the linearization is physically meaningful.

The relation of the present results to those for incidence of a concentrated single Mach wave disturbance is now briefly discussed. For two-dimensional flow, considered herein, the results of the superposition of elementary waves (as used in refs. 11 and 12) could be obtained simply by graphical construction of the Mach wave pattern. From this construction the oscillatory nature is immediately clear since for small deviations of the hot-layer boundary the Mach waves must be reflected at equal intervals. The simple reason for the exponential decay is as follows: For small disturbances the Mach numbers of the cold and hot flows are the same throughout and with them the proportionate amounts of reflection and refraction. Exponential decay results from the fact that for each repeated reflection (inside the hot layer) these proportionate amounts remain the same. The one-dimensional channel-flow approximation is also of interest. Reference to the previously derived equation for one-dimensional flow is a subsonic hot layer (eqs. (A10) to (A12)) shows that the derivation applies equally well to a supersonic hot layer. For supersonic flow in the hot layer, however, only downstream disturbances are possible; therefore equation (A12) for subsonic flow changes to

$$s = -\frac{M_{1c}^2\sqrt{M_{1h}^2 - 1}}{M_{1h}^2\sqrt{M_{1c}^2 - 1}}\, y_{1h} \tag{A19}$$

In the channel-flow approximation an oscillatory decay can, of course, not exist. The possibility of oscillatory effects are of considerable importance to the problem of reverse jet flows discussed in appendix C.

APPENDIX B

DEFORMATION OF NORMAL SHOCK AT LARGE HEIGHTS AND INFLUENCE ON SHAPE OF THROUGHGOING LAYER BEHIND SHOCK

The asymptotic deformation of the normal shock at a large height above the hot layer is calculated by a small-disturbance approach without regard to the strength of the shock and the excess temperature in the hot layer. The reason for the applicability of this approach is, as becomes apparent subsequently, that the strong deformations of the interaction pattern near the hot layer decrease to small values at large heights. The asymptotic deviation of the throughgoing hot layer as it approaches the increased thickness far behind the region of major deformation is also studied by use of the assumption of small disturbances. Griffith (ref. 6) has performed calculations for the case that the hot-layer temperature is only slightly elevated, a condition for which the small-disturbance approach applies to the complete interaction field. The present asymptotic deviation effects can, however, be singled out in such a simple fashion that their separate presentation seems worthwhile. The analysis is especially interesting because the simplicity of the approach also permits an estimate of the effect of a stagnation bubble on the shock deformation.

Shape of Shock at Large Heights

The disturbance effects influencing the normal shock at large heights can be separated into the supersonic type before the shock and the subsonic type behind it. Supersonic disturbances need not always exist at large heights inasmuch as the hot-layer flow may begin with a shock which, in turn, causes an oblique shock to be retransmitted into the flow ahead of the normal shock. The flow ahead of the shock in the hot layer and above the resulting oblique shock in the cold flow will experience no disturbance effects. If the flow in the hot layer is, however, completely subsonic, isentropic waves extend from the hot layer to an infinite distance ahead of the normal shock. At large heights above the hot layer, almost all isentropic waves will have merged into an oblique shock, but some residual waves always remain which influence the flow ahead of the shock. The decay of the supersonic disturbances at large heights ahead of the shock is determined by the decay of the disturbances in the hot layer at a large distance upstream of the shock. Since the latter decay effects are exponential, the decay with height of the supersonic disturbances before the shock is also exponential. (See fig. 19.)

The disturbance of the subsonic flow behind the normal shock is, essentially, due to an increase in thickness of the hot layer. As a consequence, it would seem proper to consider it produced by a source on the wall at the location of the dominant thickness increase; the effects of higher order singularities are negligible at large heights. Since in the present case the decay of the supersonic disturbances before the shock is of the exponential type, they can be neglected compared with the subsonic source effects behind the shock. Note that the use of potential (source) flow behind the shock is based on the assumption that the flow ahead of the normal shock can be considered undisturbed. The reason for this condition is very conveniently illustrated with the aid of the shock-polar diagram containing constant entropy lines (ref. 18, fig. 62). It is indicated that, for undisturbed flow ahead of the normal shock, the entropy lines (total-pressure lines) are tangent to the shock polars at locations presenting conditions behind the normal shock. The existence of small perturbations in the subsonic flow behind the normal shock thus produces no first-order entropy variation. The same result is presented in analytical form in reference 6.

The disturbance potential of the source flow is

$$\phi_{source} = \frac{q}{2\pi\beta} \log_e \sqrt{x^2 + \beta y^2} \tag{B1}$$

where $\beta = \sqrt{1 - M_2^2}$. The source strength q remains unspecified in the present estimate since it depends not only on the thickness increase of the hot layer but also on the distortion of the nonlinear flow field above it. The disturbance velocities in the x- and y-directions are, respectively,

$$\Delta u_2 = \frac{\partial \phi_{source}}{\partial x} = \frac{q}{2\pi\beta} \frac{x}{x^2 + \beta^2 y^2} \tag{B2}$$

and

$$\Delta v_2 = \frac{\partial \phi_{source}}{\partial y} = \frac{q}{2\pi} \frac{\beta y}{x^2 + \beta^2 y^2} \tag{B3}$$

For large heights, $y \gg x$, the following approximations can be used:

$$\Delta u_2 = \frac{bx}{\beta\left(x^2 + \beta^2 y^2\right)} \approx \frac{bx}{\beta^3 y^2} \tag{B4}$$

and

$$\Delta v_2 = \frac{b\beta y}{x^2 + \beta^2 y^2} \approx \frac{b}{\beta y} \tag{B5}$$

where $b = q/2\pi$. The disturbance velocity Δu_2 is of the order of Δv_2^2 and is thus negligibly small compared with Δv in the first-order approximation used in this development.

While a source placed along the wall will evidently satisfy the boundary condition downstream along the wall, it still has to be shown that the source flow satisfies the boundary conditions behind the shock at large heights, where the deviation from the normal is small. Since the strength of the source is not specified, only the relation between the components Δu_2 and Δv_2 has to be matched behind the shock. In other words, for the first-order approach, it is necessary to check whether Δu is negligible compared with Δv behind a shock slightly deviating from the normal. For an oblique shock the velocity components u_2 and v_2 behind the shock are related (ref. 9) as follows:

$$v_2^2 = \left(u_1 - u_2\right)^2 \frac{u_2 - \frac{u_{cr}^2}{u_1}}{\frac{u_{cr}^2}{u_1} + \frac{2}{\gamma + 1} u_1 - u_2} \tag{B6}$$

If Δv_2 and Δu_2 are designated as deviations from the components 0 and $u_{2,n}$ behind a normal shock (n refers to the normal shock), equation (B6) becomes

$$\left(\Delta v_2\right)^2 = \left[u_1 - \left(u_{2,n} + \Delta u_2\right)\right]^2 \frac{u_2 + \Delta u_2 - \frac{u_{cr}^2}{u_1}}{\frac{u_{cr}^2}{u_1} + \frac{2}{\gamma + 1} u_1 - \left(u_{2,n} + \Delta u_2\right)} \tag{B7}$$

Since for the normal shock $u_{2,n} = \frac{u_{cr}^2}{u_1}$, equation (B7) shows that Δu_2 is of the order of Δv_2^2. The velocity increment Δu is thus negligibly small compared with Δv behind the shock, as is the case for source flow; therefore, the flow field of a single source also satisfies this second boundary condition behind the shock to the first-order approximation. No higher order singularity that satisfies the boundary condition along the wall has Δu of higher order than Δv; furthermore, as already noted, the effects of higher order singularities become negligible relative to source flow at sufficiently large heights. In contrast to reference 6 (where the complete shock shape is analyzed with a small-disturbance approach), the present first-order approximation of the shock shape at large heights above the hot layer does not make it necessary to arrange a source distribution along the shock to satisfy the boundary conditions behind it.

The shape of the shock at large height above the hot layer is obtained by integrating the shock slope by use of the approximation for Δv_2 shown in equation (B5):

$$\frac{dy}{dx} = \frac{u_2 + \Delta u_2 - u_1}{\Delta v_2} \approx \frac{(u_2 - u_1)\beta}{b} y \tag{B8}$$

Integration yields a logarithmic shape for the asymptotic shock

$$x = D \log_e y + E \tag{B9}$$

when D and E are constants. The logarithmic shape of the shock as it approaches the normal at large heights above the hot layer is contained in equation (29) of reference 6.

Shape of Hot Layer Approaching Constant Height Behind Normal Shock

It was previously noted that at large heights above the hot layer the effect of its thickness increase on the normal shock can be represented by a single source since the influence of the higher order singularities are negligible at this large height. The question arises concerning the usefulness of the source in predicting the shape of the hot layer at a large distance behind the shock. For the use of such an approach, additional proof would have to be furnished that the shape of the hot layer at a large distance behind the shock is independent of the detailed nature of the dominant disturbance effects produced by the shock. (This discussion has nothing in common with that concerning the disturbance effects at large heights above the hot layer, these effects being independent of the detailed nature of the dominant disturbances.)

The independence of the hot-layer shape far behind the dominant disturbance region is plausible in view of the fact that the hot layer has a free boundary (in contrast to the fixed boundary of a solid body). This free boundary should be able to adjust itself to the hot-layer region of constant height far behind the shock, more or less independently of the detailed nature of the dominant disturbance region. Support for this plausibility consideration can be gained from the fact that the shape of the free boundary of a dead-air region far behind a body is independent of the body shape. (See ref. 5, p. 51.) In that case, where the free boundary covers a dead-air region, the asymptotic shape is a parabola. In the present case, where a source flow exists inside the (hot layer) boundary, the latter approaches the asymptotic shape of a half-body produced by a single source, the shape being a hyperbola. This can be shown in the following manner: The slope of the hot layer for small perturbations of a parallel flow is given by

$$\frac{dy}{dx} = \frac{\Delta v}{u_1}$$

The component Δv of the source flow is, according to equation (B5),

$$\Delta v = \frac{q}{2\pi} \frac{\beta y}{x^2 + \beta^2 y^2}$$

As $x \gg y$ and the hot layer approaches a constant value of y, Δv and with it the slope dy/dx become proportional to $1/x^2$. The asymptotic body shape is thus given by $y \propto 1/x$ which is a hyperbola.

This asymptotic shape of the half-body can also be obtained by applying considerations of asymptotic behavior to the small-perturbation calculations of the complete interaction field in reference 6. In reference 6, the shape of the hot-layer boundary is not determined; however, an expression for the pressure distribution is given in equation (31) or (32) of that reference. The asymptotic behavior of these equations for comparatively large values of x^* yields a pressure variation proportional to $1/x$. This result agrees with that obtained from the asymptotic small-disturbance approach for the pressure coefficient $c_p \propto \Delta u/U$. According to equation (B2)

$$\Delta u_2 = \frac{q}{2\pi} \frac{x}{x^2 + \beta^2 y^2}$$

As $x \gg y$, Δu and c_p become proportional to $1/x$.

Estimation of Effect of Bubble on Shock Deformation at Large Height

The simplicity of representation of the shock shape at large heights by means of a single source for the case of the throughgoing hot layer encourages an estimation of the effect of a stagnation bubble on the shock shape. Attempts to represent the effect of the bubble as a doublet must fail since the relation between the velocity components u and v is not that required by the boundary conditions behind the shock. A distribution of sources and sinks should, however, offer a means of satisfying both the bubble shape and the boundary conditions behind the shock at large height. In this connection, it should be noted that, depending on whether the source or the sink effects predominate, the logarithmic shock shape should approach large heights with either positive or negative distances from the bubble. The argument could be advanced, of course, that since the bubble is terminated at a finite distance, the sources and sinks would have to compensate exactly, the result being that the shock at large heights would be over the bubble. The fact that the bubble is growing, however, suggests that the source distribution

should be predominant. When a reverse jet exists under the bubble, however, a significant sink effect is introduced and the shock at large heights may be forced to extend to negative logarithmic infinity. In other words, the shock may have to pull the layer along rather than push it as is the case when it extends to positive infinity.

APPENDIX C

QUASI-STEADY FLOW STABILITY OF COUNTERFLOWING REVERSE JET MOVING UNDER HOT LAYER

When the reverse jet is permitted to extend fully under the hot layer, it has to match the pressure of the undisturbed state; and, as a result, the jet approaches the supersonic Mach number of the cold flow if constant entropy is assumed. The question arises as to whether this counterflowing supersonic reverse jet can exist in the presence of the supersonic unlimited flow separated from it by the hot layer. The existence of this quasi-steady triple-layer pattern is tested by studying its stability to small steady disturbances. (See figs. 9 and 10(b).)

The disturbance potential of the supersonic unlimited flow over the hot layer is, as in equations (A1) and (A13),

$$\phi_c = u_1 C e^{\frac{1}{s}\left(x - y\sqrt{M_{1c}^2 - 1}\right)} \qquad (y_{cj} + y_{lh} < y < \infty) \qquad (C1)$$

The Mach number of the flow is M_{1c}, and the heights of the reverse jet and the hot layer y_{cj} and y_{lh}, respectively. The equation for the hot-layer flow, however, differs slightly from equations (A2) or (A14) for subsonic or supersonic hot-layer flow. (The subsonic case is used as an example.) The reason for this difference is that the lower hot-layer boundary is no longer the wall, but the upper boundary of the reverse jet. As a consequence, from the formal viewpoint it would seem to be necessary to express the potential ϕ_h in two terms as

$$\phi_h = u_1 F e^{x/s} \cos\left(\frac{y}{s}\sqrt{1 - M_{1h}^2}\right) + u_1 G e^{x/s} \sin\left(\frac{y}{s}\sqrt{1 - M_{1h}^2}\right)$$

where the second term enables a matching of the flows at the now free lower boundary of the hot layer. However, it is more convenient to combine the two terms by introducing a phase shift β in the first

term, since β can be made to drop out in the final analysis. The disturbance potential of the hot-layer flow is thus expressed in the form

$$\phi_h = u_1 C^* e^{x/s} \cos\left(\frac{y}{s}\sqrt{1 - M_{1h}^2} + \beta\right) \qquad \left(y_{cj} < y < y_{cj} + y_{1h}\right) \tag{C2}$$

The following disturbance potential of the supersonic reverse jet flow is of the same form as that of a supersonic hot-layer flow moving in the same direction as the unlimited supersonic flow (eq. (A14)):

$$\phi_{cj} = u_1 C^{**} e^{x/s} \cosh\left(\frac{y}{s}\sqrt{M_{cj}^2 - 1}\right) \qquad \left(0 < y < y_{cj}\right) \tag{C3}$$

The independence of the flow direction can be most conveniently seen in equation (C12) for the triple-layer interaction where the constants have been eliminated. The flow direction in that equation appears only in the Mach number M_{cj} which, however, occurs only as a squared term.

The slopes of the streamlines of the three flows are

$$\frac{1}{u_1}\left(\frac{\partial \phi_c}{\partial y}\right) = -C\,\frac{1}{s}\sqrt{M_{1c}^2 - 1}\; e^{\frac{x}{s}} e^{-\frac{y}{s}\sqrt{M_{1c}^2 - 1}} \tag{C4}$$

$$\frac{1}{u_1}\left(\frac{\partial \phi_h}{\partial y}\right) = -C^*\,\frac{1}{s}\sqrt{1 - M_{1h}^2}\; e^{x/s} \sin\left(\frac{y}{s}\sqrt{1 - M_{1h}^2} + \beta\right) e^{x/s} \tag{C5}$$

$$\frac{1}{u_1}\left(\frac{\partial \phi_{cj}}{\partial y}\right) = C^{**}\,\frac{1}{s}\sqrt{M_{cj}^2 - 1}\; e^{x/s} \sinh\left(\frac{y}{s}\sqrt{M_{cj}^2 - 1}\right) \tag{C6}$$

The respective pressure increments are

$$\frac{\gamma M_{1c}^2}{u_1}\left(\frac{\partial \phi_c}{\partial x}\right) = C\gamma M_{1c}^2\,\frac{1}{s}\, e^{\frac{x}{s}} e^{-\frac{y}{s}\sqrt{M_{1c}^2 - 1}} \tag{C7}$$

$$\frac{\gamma M_{1h}^2}{u_1}\left(\frac{\partial \phi_h}{\partial x}\right) = C^*\gamma M_{1h}^2 \frac{1}{s} e^{x/s}\cos\left(\frac{y}{s}\sqrt{1 - M_{1h}^2} + \beta\right) \tag{C8}$$

$$\frac{\gamma M_{cj}^2}{u_1}\left(\frac{\partial \phi_{cj}}{\partial x}\right) = C^{**}\gamma M_{cj}^2 e^{x/s}\cosh\left(\frac{y}{s}\sqrt{M_{cj}^2 - 1}\right) \tag{C9}$$

Equating the respective slopes and pressures at the upper and lower hot-layer boundaries $\left(y = y_{cj} + y_{1h} \text{ and } y = y_{cj}\right)$ and equating the resulting ratios of coefficients yield two equations:

$$\beta + \frac{y_{cj} + y_h}{s}\sqrt{1 - M_{1h}^2} = \tan^{-1}\frac{M_{1h}^2\sqrt{M_{1c}^2 - 1}}{M_{1c}^2\sqrt{1 - M_{1h}^2}} \tag{C10}$$

$$\beta + \frac{y_{cj}}{s}\sqrt{1 - M_{1h}^2} = -\tan^{-1}\left[\frac{M_{1h}^2\sqrt{M_{cj}^2 - 1}}{M_{cj}^2\sqrt{1 - M_{1h}^2}}\tanh\left(\frac{y_{cj}}{s}\sqrt{M_{cj}^2 - 1}\right)\right] \tag{C11}$$

Elimination of the phase shift β by subtraction yields:

$$\frac{y_{1h}}{s}\sqrt{1 - M_{1h}^2} = \tan^{-1}\frac{M_{1h}^2\sqrt{M_{1c}^2 - 1}}{M_{1c}^2\sqrt{1 - M_{1h}^2}} + \tan^{-1}\left[\frac{M_{1h}^2\sqrt{M_{cj}^2 - 1}}{M_{cj}^2\sqrt{1 - M_{1h}^2}}\tanh\left(\frac{y_{cj}}{s}\sqrt{M_{cj}^2 - 1}\right)\right] \tag{C12}$$

Equation (C12) reduces to equation (A7) for the interaction with a single subsonic hot layer if the thickness y_{cj} of the reverse jet is set equal to zero. The results for the interaction with a single supersonic hot layer (eqs. (A15) and (A16)) are obtained by setting the thickness y_{1h} of the subsonic hot layer equal to zero and by replacing M_{cj} with M_{1h}.

Since equation (C12) is of the complex transcendental type in the unknown complex decay modulus s, its direct solution cannot be obtained without performing lengthy calculations. Physical reasoning, combined with inspection of equation (C12), however, permits gaining sufficient understanding of the solutions for the present exploratory purpose.

It is noted in the body of the paper that the reverse jet, being part of the flow pattern around the bubble, has to experience the same quasi-steady growth of its height. The undisturbed hot-layer region under which the reverse jet flows, however, does not participate in this growth. Thus, after some time of quasi-steady growth the height of the undisturbed hot-layer region y_{lh} will be small compared with the height of the reverse jet y_{cj}. As a matter of fact, the quasi-steady state of this study is better satisfied as larger values of y_{cj} are compared with y_{lh}. In view of this nature of the limiting quasi-steady state, it appears permissible to consider the actual triple-layer steady stability problem as a double-layer stability problem with a few appropriate corrections.

If the hot layer is neglected then for the moment, the simple problem of the stability of a supersonic jet or layer of finite height moving counter to the unlimited supersonic flow adjacent to it can be considered. It was previously noted that the equations do not change when the flow direction in the jet is changed. However, since the direction of the jet flow is opposite to the direction of the unlimited flow, a decrease in the deviation from the horizontal of its boundary in the direction of the unlimited flow will mean an increase of this same deviation in the direction of the reverse jet flow. (The fact that for the interaction of an unlimited supersonic flow with one of finite height the disturbances can decay only in the downstream direction - only negative values of s exist - of the unlimited flow has already been established in appendix A). The supersonic reverse jet is thus not stable in the steady sense to small disturbances for the limiting case of the negligibly thin hot layer; that is, the two opposed supersonic flows cannot exist together if small disturbances are superimposed. The hot layer between the two counterflowing streams will produce some damping of the disturbances; however, in view of its comparatively small height, these effects are not likely to be large enough to prevent instability of the steady reverse-jet flow. Any damping in the reverse jet will then, most probably, be of the nonlinear type; that is, it must result from the entropy increase through shocks of finite strength. That such damping should eventually occur appears likely because the disturbances are predominantly of the oscillatory type, as indicated by the previous solution for the limiting case of the interaction where the hot layer is negligibly thin. An oscillatory flow in the reverse jet includes a large number of concave boundary

sections which cause shock formations and damping of the large amplitude deviations through entropy increase. The entropy increase causes the Mach number in the reverse jet to approach 1. Since the amplitudes of the oscillations become small as a Mach number of 1 is approached, the small-disturbance approach may be used again.

In the limiting case of the negligibly thin hot layer, the analysis in appendix A applies where the interaction of a finite and an unlimited supersonic stream is considered. (M_{1h} in appendix A has to be replaced by M_{cj}.) Appendix A shows that, as M_{cj} approaches 1, the decay modulus σ approaches a finite negative value whereas the wavelength λ approaches zero. Setting $M_{cj} = 1$ in equation (C12), which includes the effect of the hot layer, however, cancels the term due to reverse-jet influence; this fact means that the reverse jet is no longer a destabilizing influence. To be precise, if the ratio y_{cj}/s does not approach infinity as $M_{cj}^2 - 1$ approaches zero, the second right-hand term in equation (C12) is zero. A detailed study of the problem lies, however, beyond the scope of this paper, especially since it would require more knowledge about the nonlinear damping effects.

Finally, a check of equation (C12) is made, based on the one-dimensional channel-flow approach. (This check will again indicate the restrictive nature of this simple approach.) The relative pressure change in the subsonic hot layer is

$$\frac{\Delta p}{p_1} = \frac{\gamma M_{1h}^2}{1 - M_{1h}^2} \frac{\Delta y_{1h}}{y_{1h}} \tag{C13}$$

The pressure decrease of the supersonic reverse jet with increasing cross section is

$$\frac{\Delta p}{p_1} = - \frac{\gamma M_{cj}^2}{M_{cj}^2 - 1} \frac{\Delta y_{cj}}{y_{cj}} \tag{C14}$$

The relative pressure increase $\Delta p/p_1$ may be expressed in terms of the cross-sectional variation of the combined layers by using the fact that, if $\frac{a}{b} = \frac{c}{d}$, the ratios are also equal to $\frac{a + c}{b + d}$. Thus,

$$\frac{\Delta p}{p_1} = \frac{\gamma M_{1h}^2 M_{cj}^2 (\Delta y_{1h} + \Delta y_{cj})}{y_{1h}\left(1 - M_{1h}^2\right)M_{cj}^2 - y_{cj}\left(M_{cj}^2 - 1\right)M_{1h}^2} \tag{C15}$$

The relative pressure increase for the unlimited supersonic flow over the hot layer is

$$\frac{\Delta p}{p_1} = \frac{\gamma M_{1c}^2}{\sqrt{M_{1c}^2 - 1}} \frac{d\left(\Delta y_{1h} + \Delta y_{cj}\right)}{dx} \tag{C16}$$

Equating (C15) and (C16) gives

$$\frac{d\left(\Delta y_{1h} + \Delta y_{cj}\right)}{dx} = \frac{\sqrt{M_{1c}^2 - 1}}{M_{1c}^2} \frac{M_{1h}^2 M_{cj}^2 \left(\Delta y_{1h} + \Delta y_{cj}\right)}{y_{1h}\left(1 - M_{1h}^2\right)M_{cj}^2 - y_{cj}\left(M_{cj}^2 - 1\right)M_{1h}^2} \tag{C17}$$

Then, for the subtangent or the decay modulus s

$$s = \frac{\Delta y_{1h} + \Delta y_{cj}}{\frac{d\left(\Delta y_{1h} + \Delta y_{cj}\right)}{dx}}$$

$$= \frac{y_{1h}\left(1 - M_{1h}^2\right)M_{cj}^2 - y_{cj}\left(M_{cj}^2 - 1\right)M_{1h}^2}{M_{1h}^2 \sqrt{M_{1c}^2 - 1}} \frac{M_{1c}^2}{M_{cj}^2} \tag{C18}$$

Equation (C12) for the two-dimensional interaction problem reduces to equation (C18) under the conditions that the $\tanh^{-1}(\ )$ and the $\tan^{-1}(\ )$ terms can be replaced by their arguments. The substitution yields

$$\frac{y_{1h}}{s}\sqrt{1 - M_{1h}^2} = \frac{M_{1h}^2 \sqrt{M_{1c}^2 - 1}}{M_{1c}^2 \sqrt{1 - M_{1h}^2}} + \frac{M_{1h}^2\left(M_{cj}^2 - 1\right)}{M_{cj}^2 \sqrt{1 - M_{1h}^2}} \frac{y_{cj}}{s}$$

which can be rearranged to agree with equation (C18). It is indicated, as presumed, that the one-dimensional channel-flow approximation applies only to large values of the decay modulus s. Thus, while it is tempting to look for a simple one-dimensional criterion for the steady stability

problem in equation (C18), based on the predominance of the positive or the negative term, it has to be resisted inasmuch as small values of s no longer belong to the one-dimensional channel-flow approximation. Also, the stability test of the reverse-jet flow involves largely oscillatory amplifications, which certainly cannot be represented by the channel-flow approximation.

REFERENCES

1. Jahn, Robert G.: The Refraction of Shock Waves at a Gaseous Interface - III. Irregular Refraction. Tech. Rep. II-19 (Contract N6ori-105, Task II), Princeton Univ., Dept. Phys., Apr. 1955.

2. Griffith, Wayland C., and Bleakney, Walker: Diffusion Analogy to Interaction of a Shock With a Thermal Boundary Layer. Tech. Rep. II-17 (Contract N6ori-105, Task II), Princeton Univ., Dept. Phys., Jan. 1955.

3. Friedrichs, K. O., and Keller, Joseph B.: Geometrical Acoustics. II. Diffraction, Reflection, and Refraction of a Weak Spherical or Cylindrical Shock at a Plane Interface. Jour. Appl. Phys., vol. 26, no. 8, Aug. 1955, pp. 961-966.

4. Guderley, K. Gottfried: Considerations of the Structure of Mixed Subsonic-Supersonic Flow Patterns. Tech. Rep. No. F-TR-2168-ND, Air Materiel Command, U. S. Air Force, Oct. 1947.

5. Birkhoff, Garrett: Hydrodynamics. Princeton Univ. Press, 1950.

6. Griffith, Wayland C.: Interaction of a Shock Wave With a Thermal Boundary Layer. Jour. Aero. Sci., vol. 23, no. 1, Jan. 1956, pp. 16-22, 66.

7. Hess, Robert V.: Study of Unsteady Flow Disturbances of Large and Small Amplitudes Moving Through Supersonic or Subsonic Steady Flows. NACA TN 1878, 1949.

8. Liepmann, Hans Wolfgang, and Puckett, Allen E.: Introduction to Aerodynamics of a Compressible Fluid. John Wiley & Sons, Inc., 1947.

9. Ferri, Antonio: Elements of Aerodynamics of Supersonic Flows. The Macmillan Co., 1949.

10. Tsien, H. S., and Finston, M.: Interaction Between Parallel Streams of Subsonic and Supersonic Velocities. Jour. Aero. Sci., vol. 16, no. 9, Sept. 1949, pp. 515-528.

11. Pai, S. I.: On Supersonic Flow of a Two-Dimensional Jet in Uniform Stream. Jour. Aero. Sci., vol. 19, no. 1, Jan. 1952, pp. 61-65.

12. Pack, D. C.: The Oscillations of a Supersonic Gas Jet Embedded in a Supersonic Stream. Jour. Aero. Sci., vol. 23, no. 8, Aug. 1956, pp. 747-753, 764.

13. Stewart, George Walter, and Lindsay, Robert Bruce: Acoustics. D. Van Nostrand Co., Inc., 1930.

14. Hollyer, Robert N., Jr.: A Study of Attenuation in the Shock Tube. Project M720-4 (Contract No. N6-ONR-232-TO IV), Eng. Res. Inst., Univ. of Michigan, July 1953.

15. Trimpi, Robert L., and Cohen, Nathaniel B.: A Theory for Predicting the Flow of Real Gases in Shock Tubes With Experimental Verification. NACA TN 3375, 1955.

16. Mirels, Harold: Laminar Boundary Layer Behind Shock Advancing Into Stationary Fluid. NACA TN 3401, 1955.

17. Shapiro, Ascher H.: The Dynamics and Thermodynamics of Compressible Fluid Flow. Vol. I. The Ronald Press Co., c.1953, p. 582.

18. Busemann, A.: Gas Dynamics. Part IV. Two-Dimensional Flows. R.T.P. Trans. No. 2210, British Ministry of Aircraft Production. (Handbuch der Experimentalphysik., vol. 4. Wien-Harms, 1931, pp. 407-442.

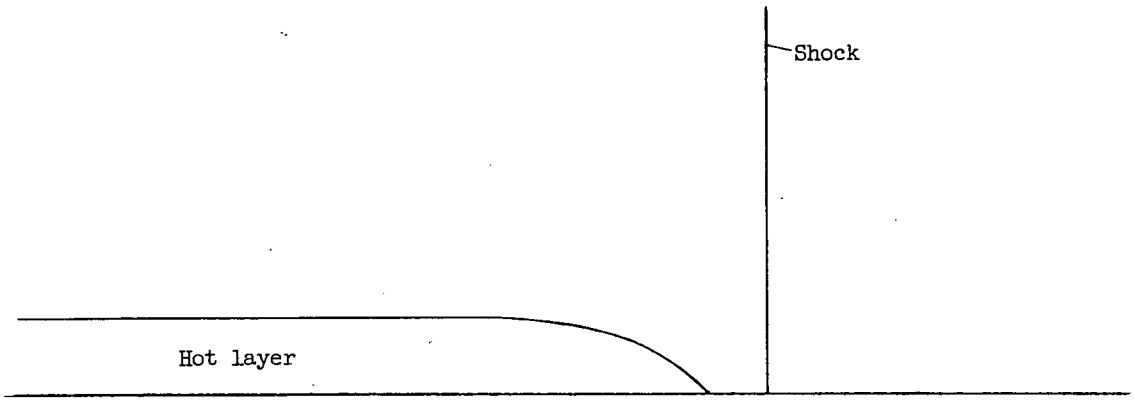

Figure 1.- Hot layer and shock before interaction.

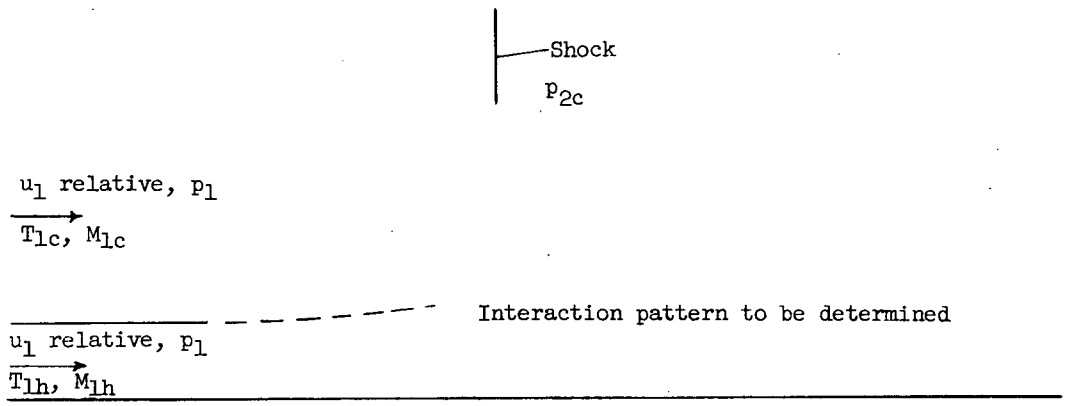

Known: Strength of shock expressed through relative $M_{1c} = \frac{u_1}{a_{1c}}$

Temperature ratio, $\frac{T_{1h}}{T_{1c}}$

Relative $M_{1h}^2 = M_{1c}^2 \frac{T_{1c}}{T_{1h}}$

Figure 2.- Flow system relative to shock for analysis of interaction patterns.

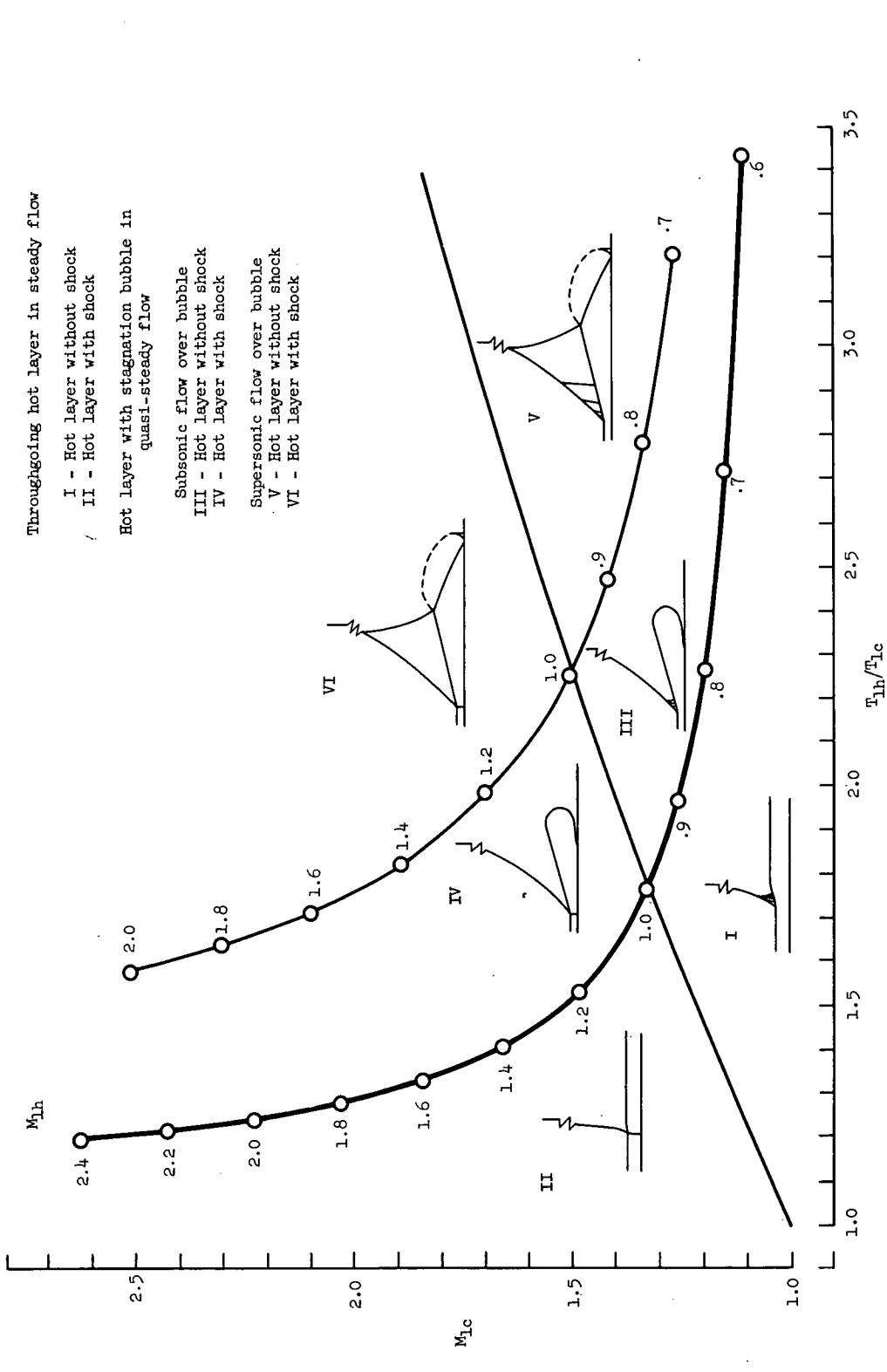

Figure 3.- Six major types of flow patterns in terms of shock strength M_{1c} and temperature ratio T_{1h}/T_{1c}.

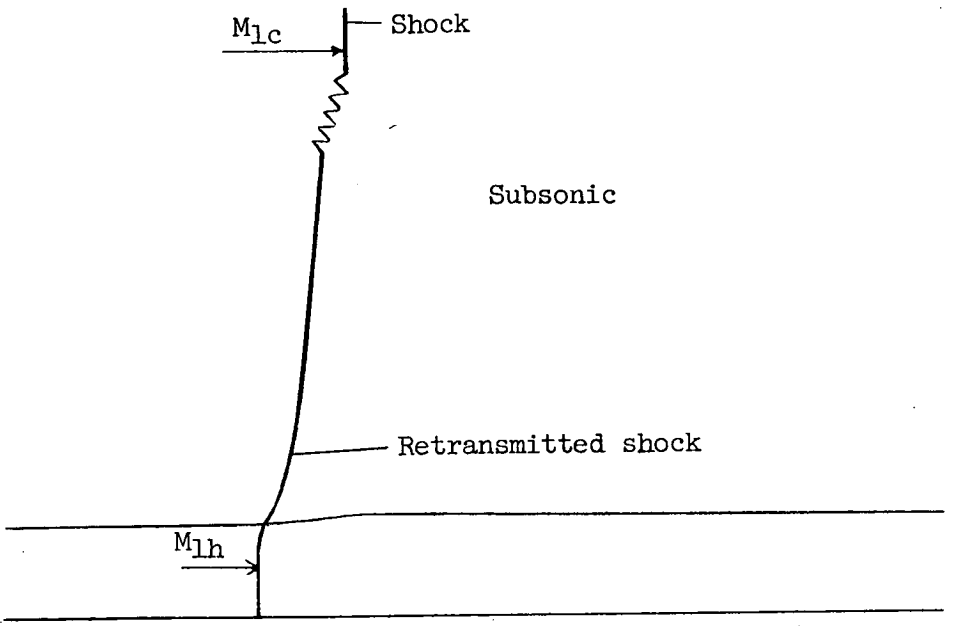

Figure 4.- Throughgoing hot layer with subsonic compression behind retransmitted shock.

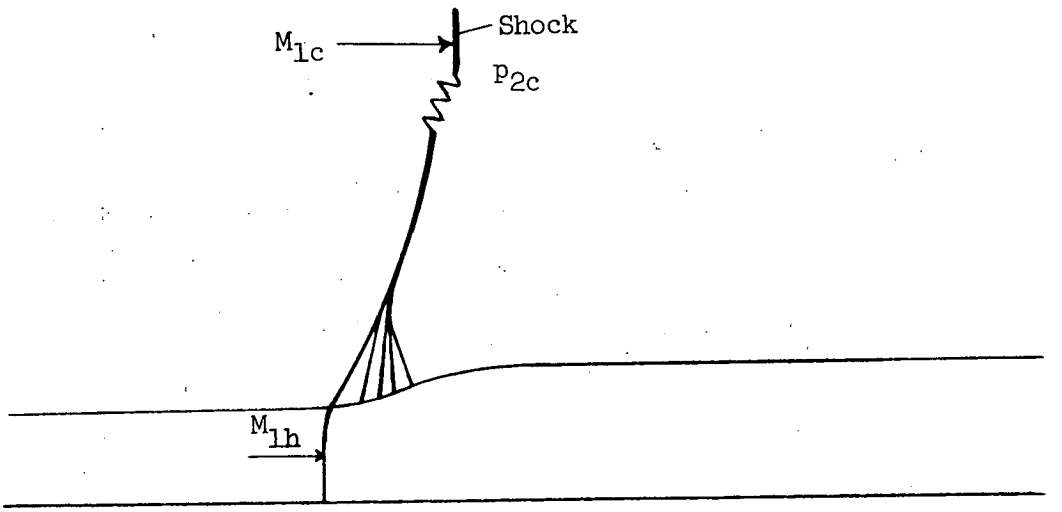

Figure 5.- Throughgoing hot layer with supersonic and subsonic compressions behind retransmitted shock.

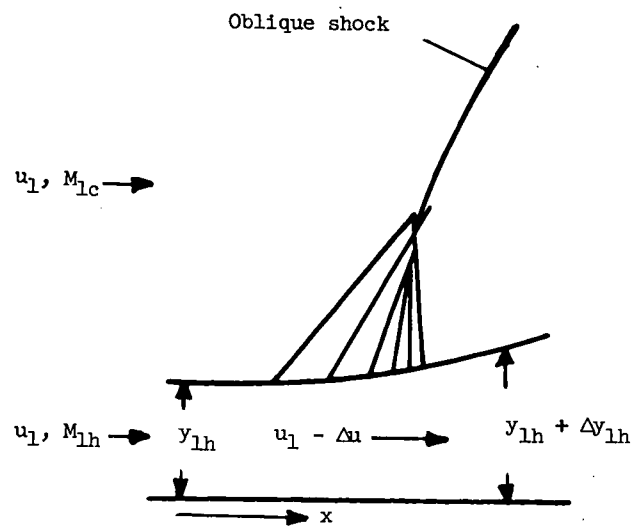

Figure 6.- Upstream decay of compression effects.

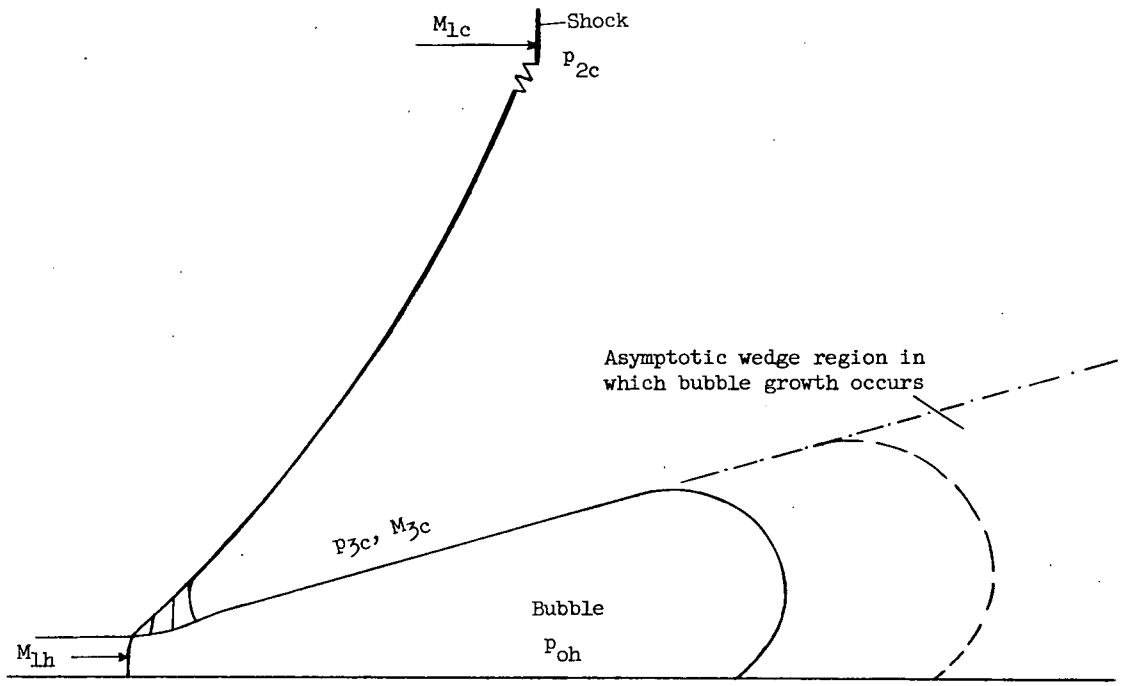

Figure 7.- Hot layer terminated by stagnation bubble with quasi-steady growth. Rise to stagnation pressure in hot layer is less than jump of pressure through shock.

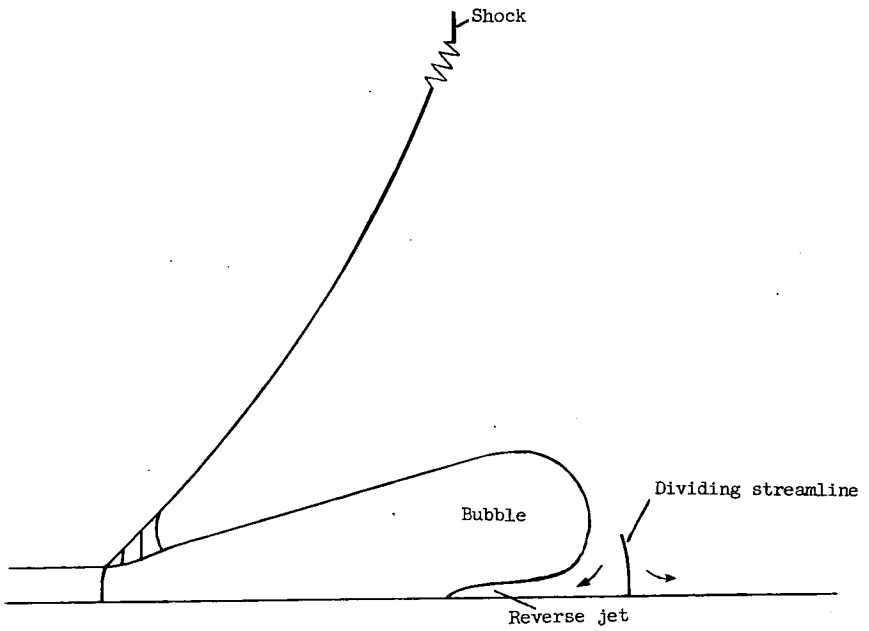

(a) Reverse jet does not break into bubble.

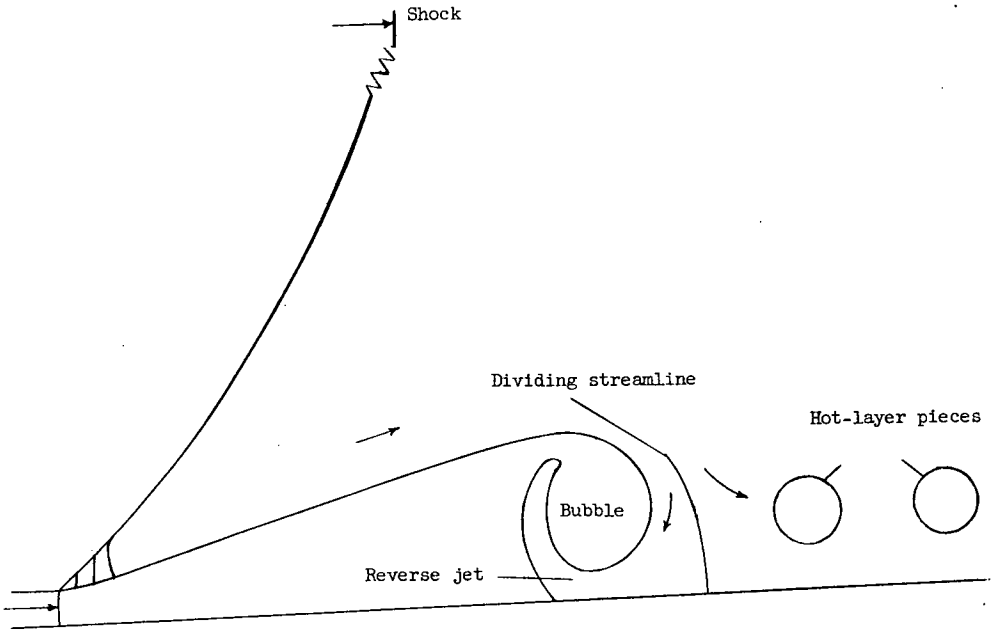

(b) Picture of what would happen if reverse jet broke into stagnation bubble without waiting for influence of real-flow effects.

Figure 8.- Progress of reverse jet under bubble.

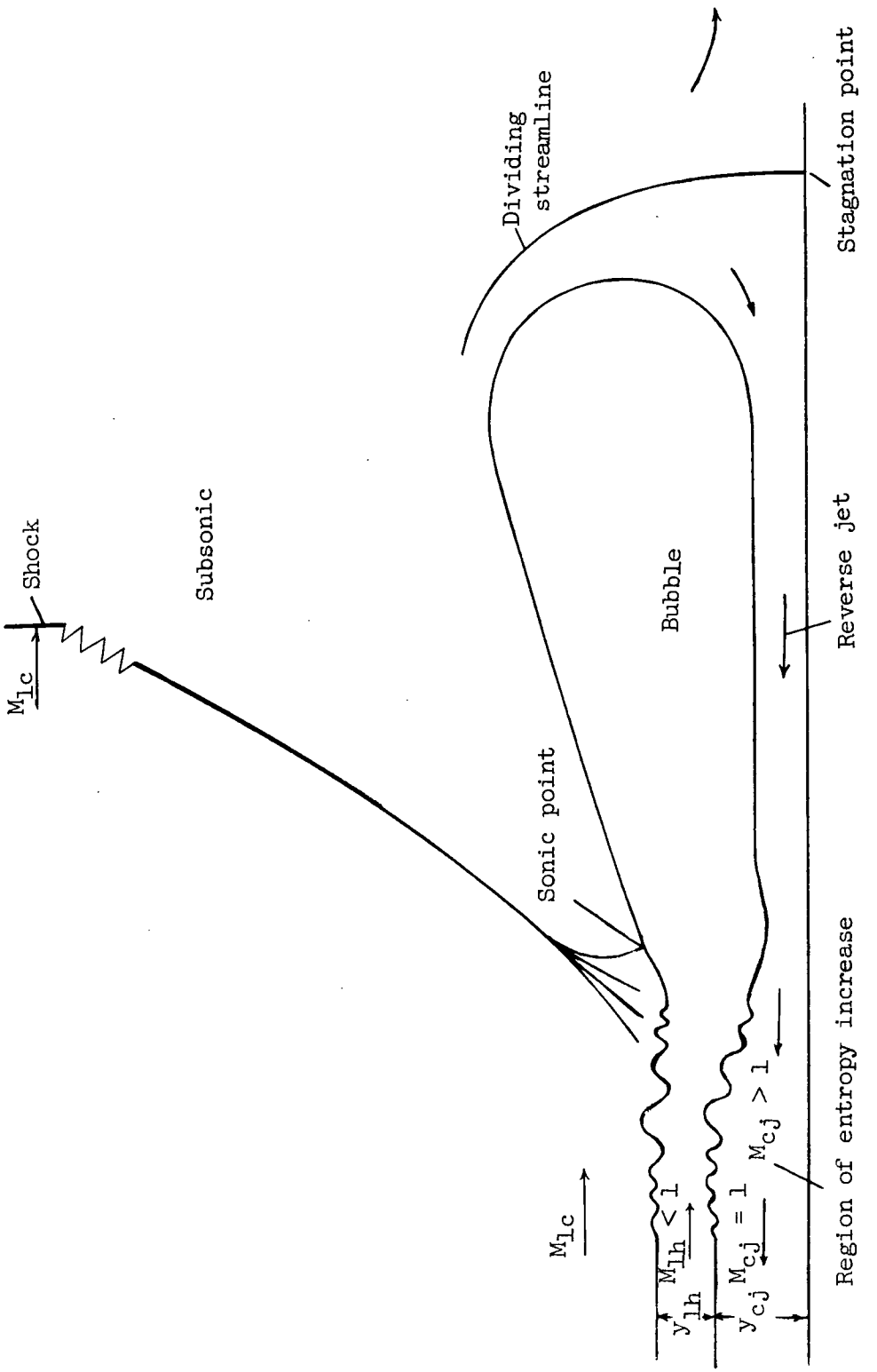

Figure 9.- Subsonic flow over bubble with reverse jet.

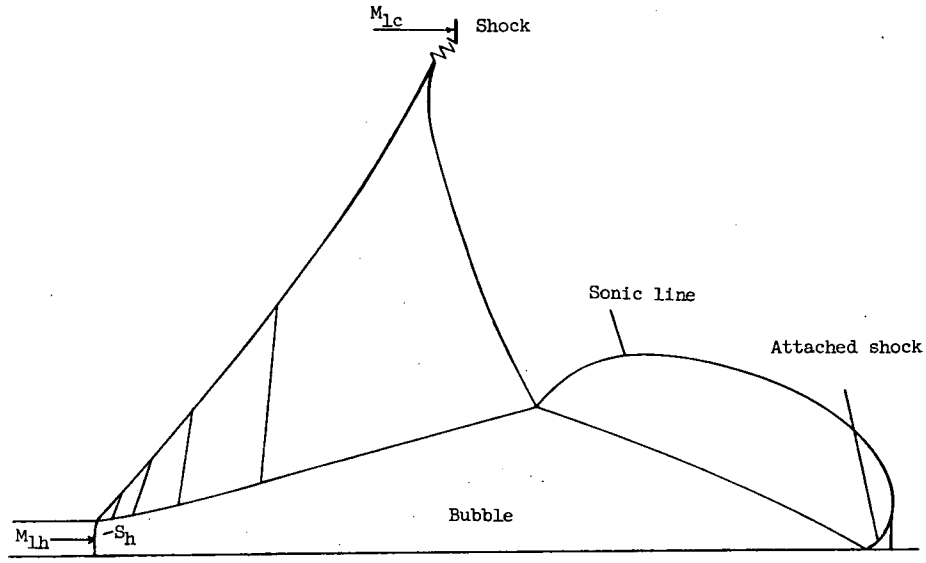

(a) With shock attached at base.

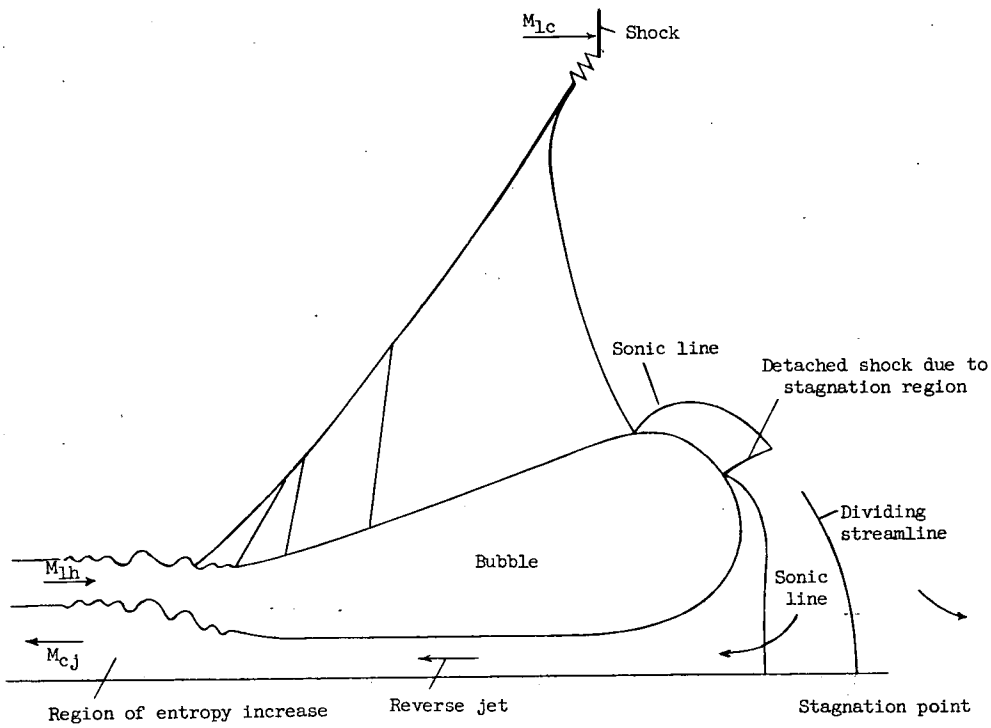

(b) With reverse jet.

Figure 10.- Tentative supersonic flow over bubble.

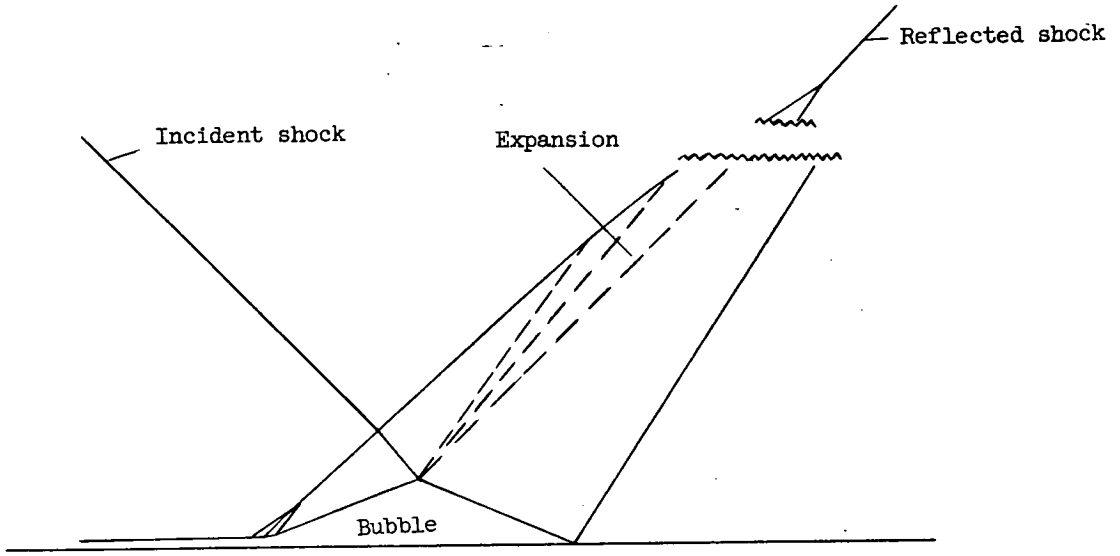

Figure 11.- Oblique-shock interaction with bubble formation.

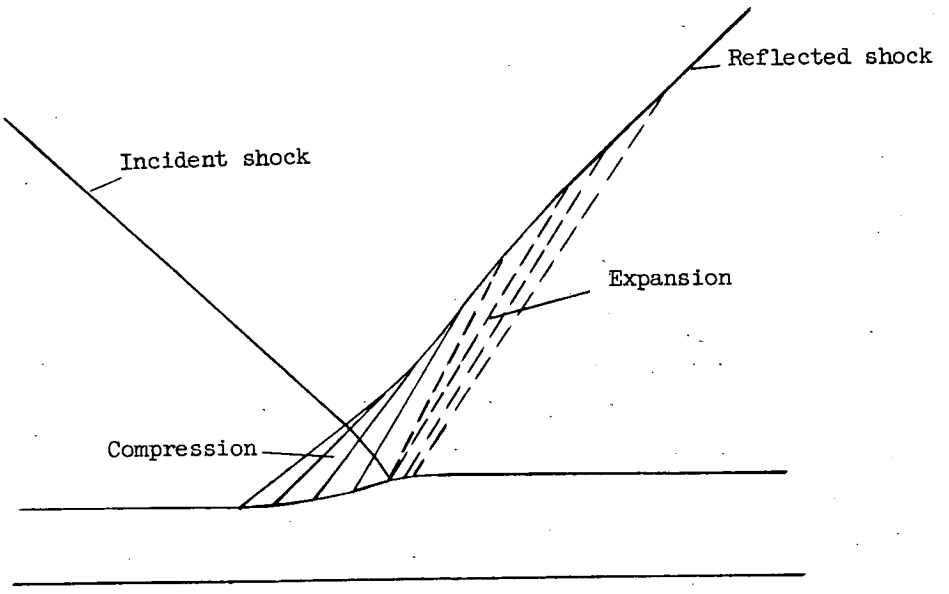

Figure 12.- Oblique-shock interaction with throughgoing subsonic hot layer.

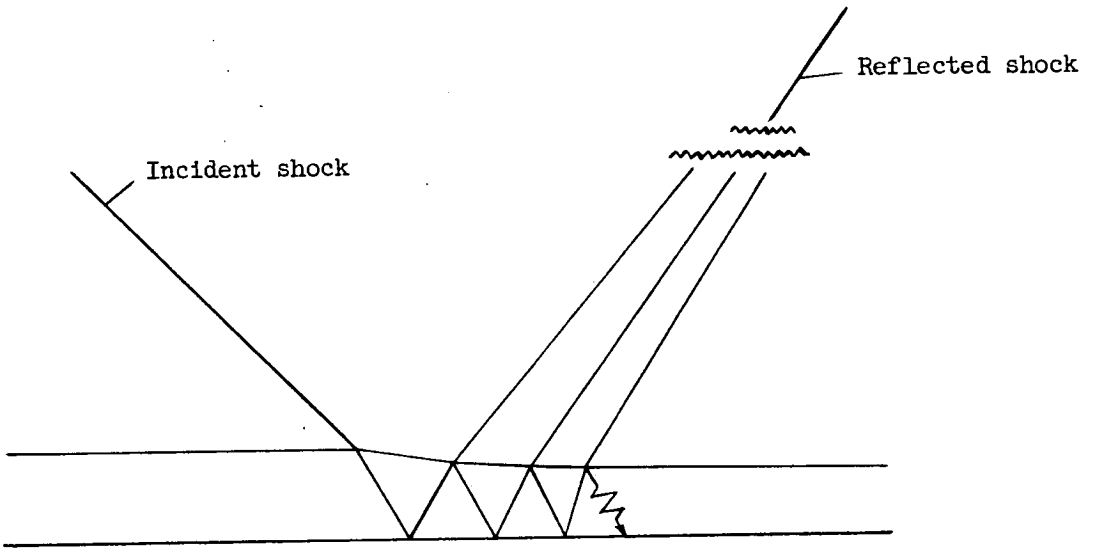

(a) Showing repeated reflection.

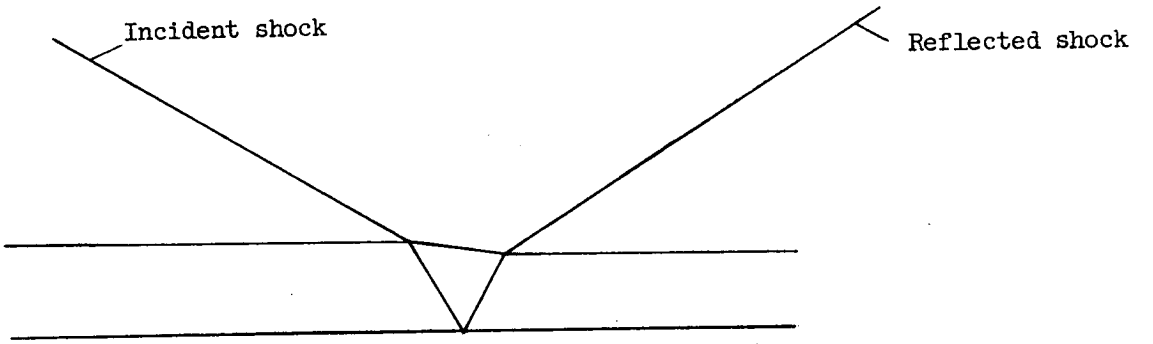

(b) Showing single reflection.

Figure 13.- Oblique-shock interaction pattern with supersonic flow in hot layer.

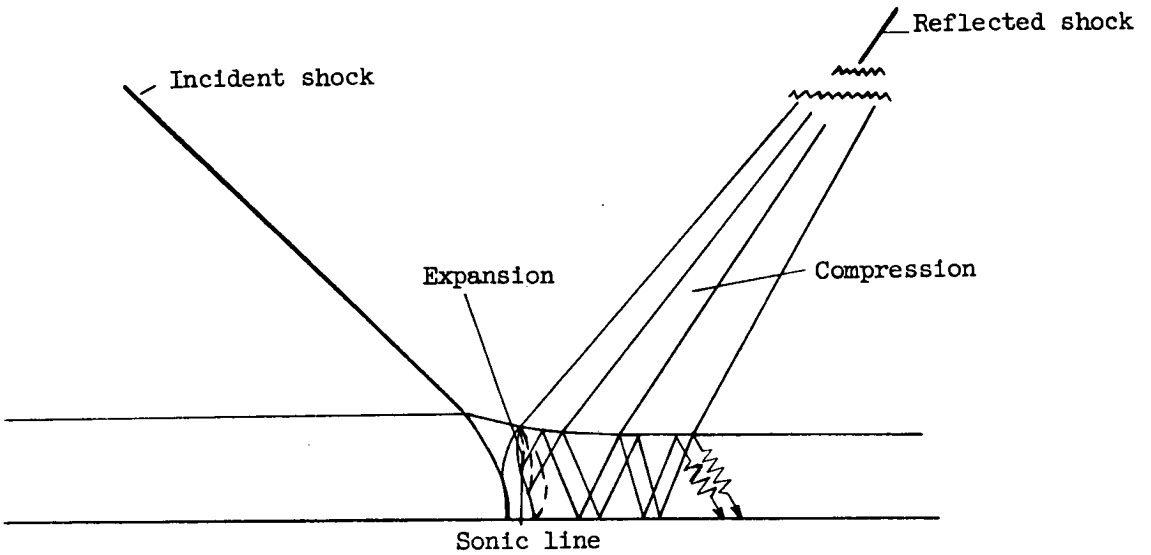

Figure 14.- Oblique-shock interaction pattern with Mach stem followed by repeated reflections in hot layer.

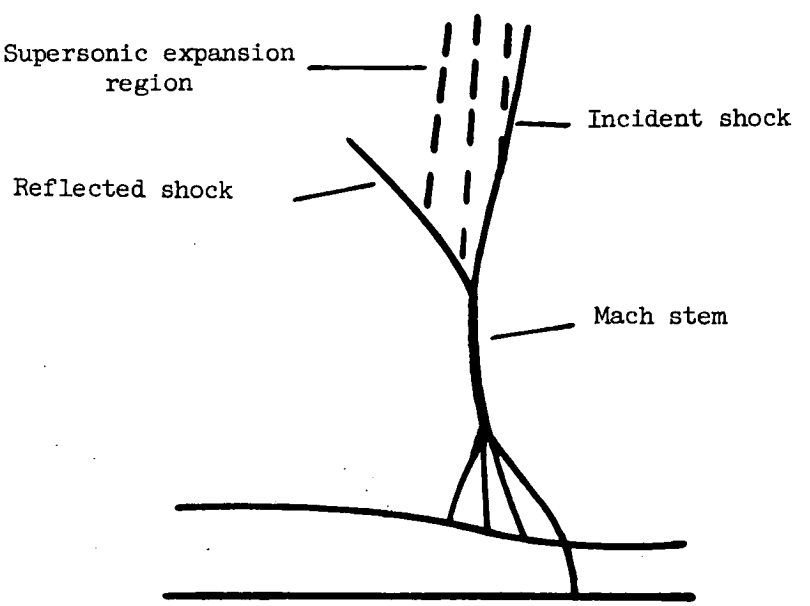

Figure 15.- Cylindrical-shock interaction with Mach stem over hot layer.

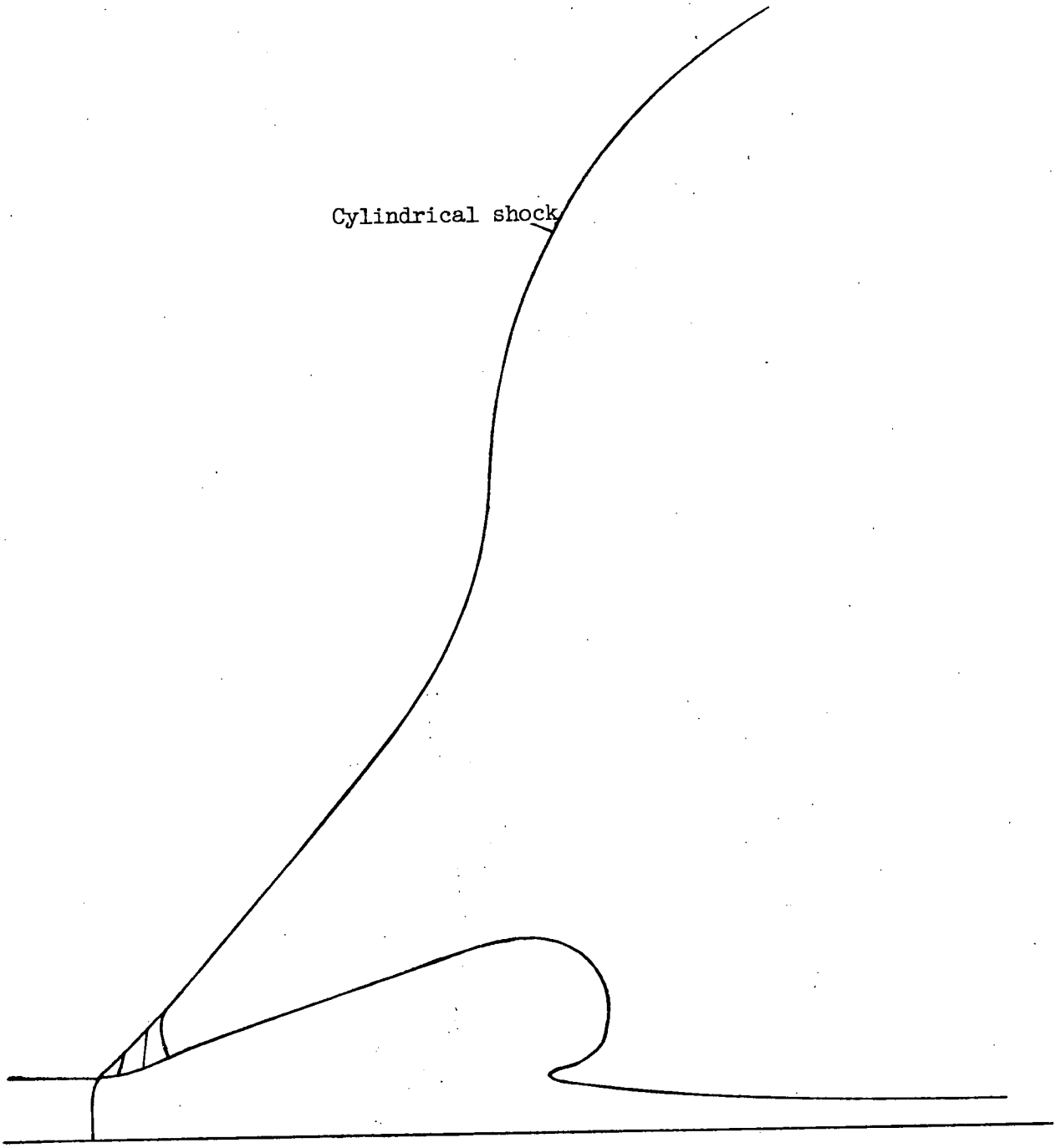

Figure 16.- Tentative interaction pattern of cylindrical shock and hot layer with bubble formation.

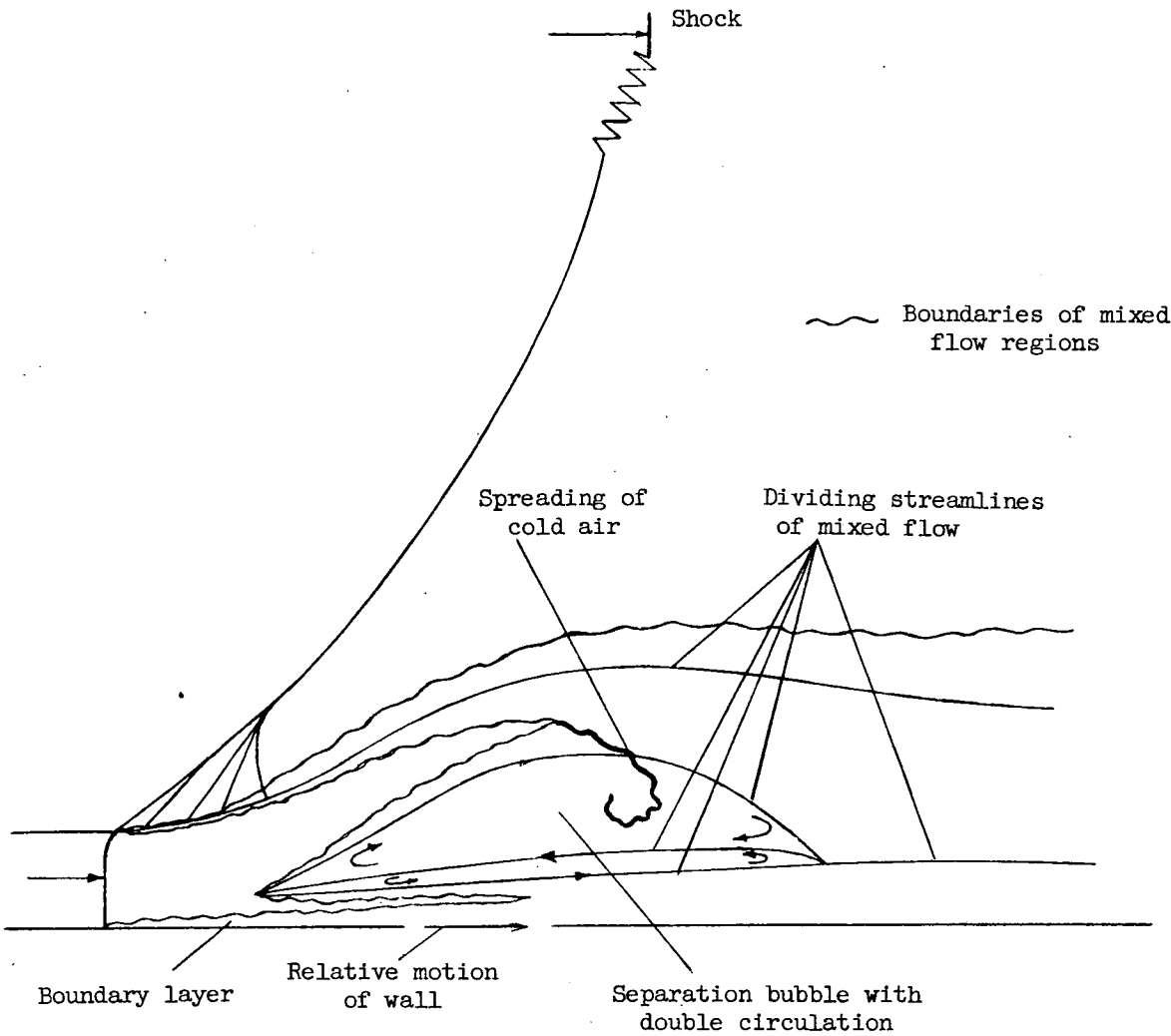

Figure 17.- Tentative mixed-flow pattern with subsonic flow over separation bubble.

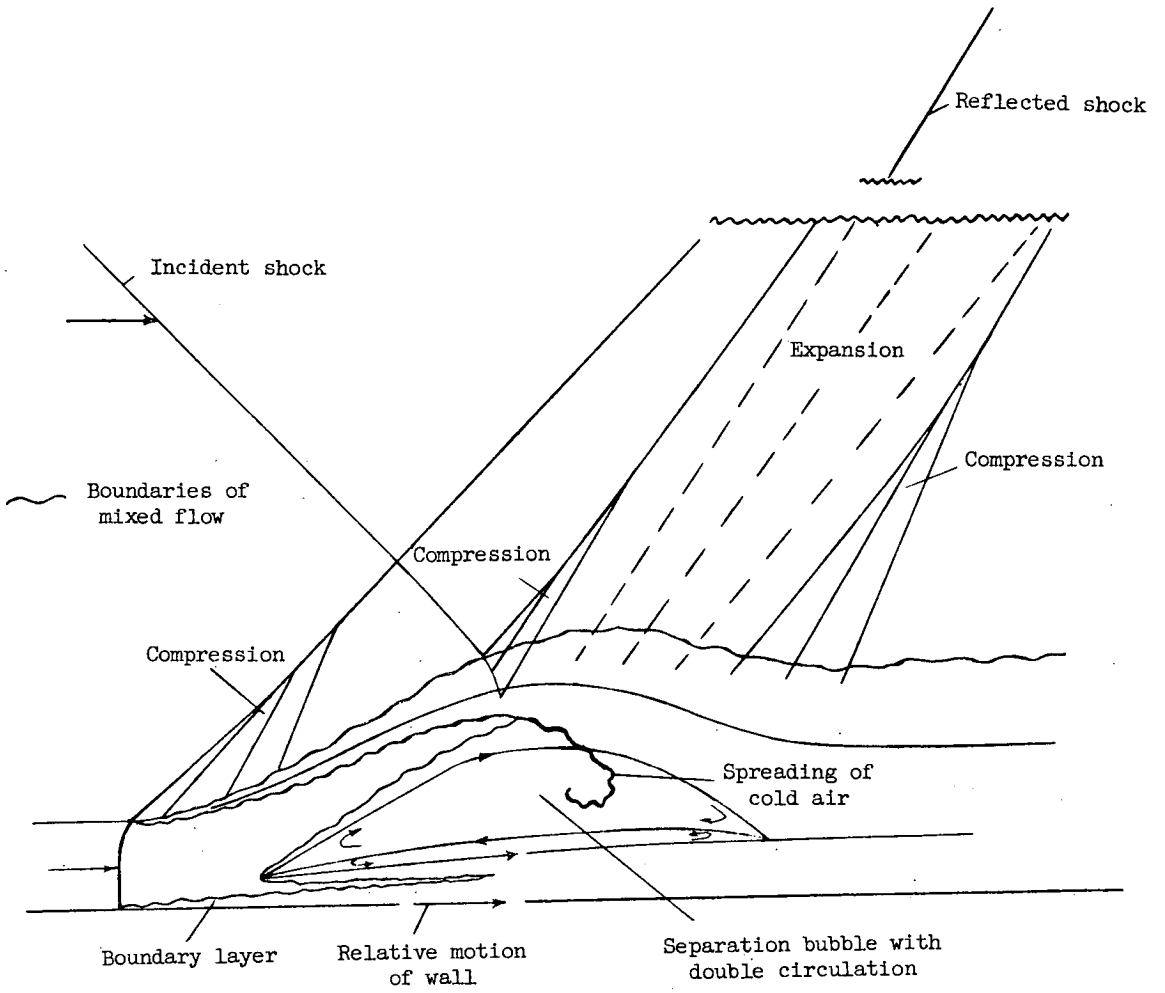

Figure 18.- Tentative mixed-flow pattern with supersonic flow over separation bubble.

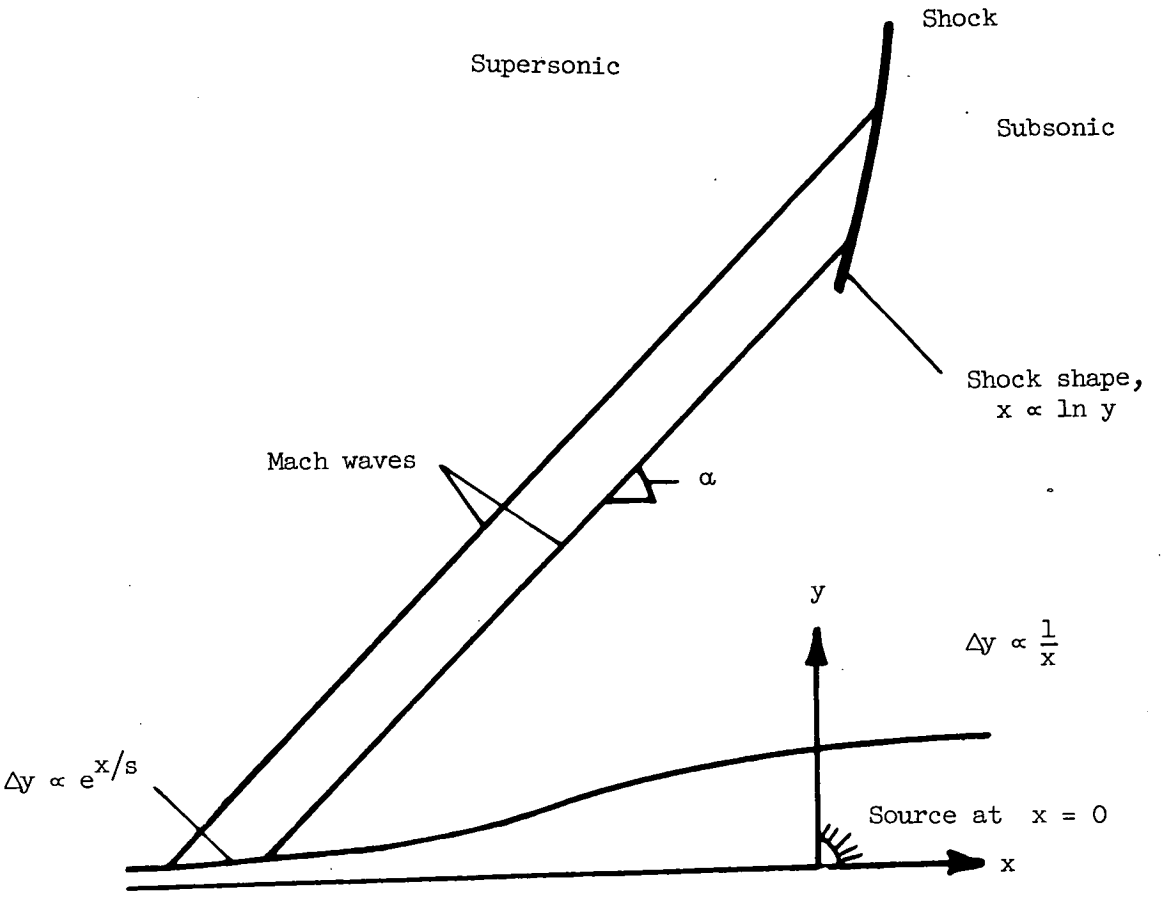

Figure 19.- Calculation of asymptotic shock shape.